The Pennsylvania State University

The Graduate School

Department of Bioengineering

REAL-TIME FEEDBACK IN A VOLUMETRIC DISPLAY FOR MOTOR LEARNING APPLICATIONS

A Thesis in

Bioengineering

by

John Robert Miller

Submitted in Partial Fulfillment
of the Requirements
for the Degree of

Master of Science

May 2016

The thesis of John Miller was reviewed and approved* by the following:

Stephan J. Piazza
Professor of Kinesiology
Thesis Advisor

Keefe Manning
Associate Professor of Biomedical Engineering

Peter Butler
Professor of Biomedical Engineering

William Hancock
Professor of Biomedical Engineering
Head of the Bioengineering Graduate Program

*Signatures are on file in the Graduate School

ABSTRACT

The goal of this thesis is to develop a volumetric display for portraying human body motions in real-time. The results of three-dimensional motion analyses are typically displayed on a two-dimensional video screen. While such views may be rotated to give the appearance of a three dimensional motion, viewing a flat screen is inherently different from a truly three-dimensional display. A volumetric display would allow perception of the motion in three true dimensions and multiple observers could simultaneously view the same motion from different angles. Two different approaches to volumetric displays were explored, an LED display and a projected-light string display. The former is controlled by a microcontroller that is programmed to light a 3-D array of LEDs, and the latter involves projection of a two-dimensional image onto an array of vertical strings to create the three-dimensional image. Because it was less expensive to fabricate and easier to interface with the motion capture system, it was decided to move forward with the projected-light string display. Using a six camera Eagle Motion System, the coordinates of markers placed on human body segments were recorded and accessed in MATLAB in real-time. The marker data were used to calculate intersections between the body segments and the strings in the display. These intersections were represented as rectangles in a two-dimensional image projected onto the strings to create the three-dimensional image. Three applications were developed to demonstrate the capabilities of the display: (1) real-time posture assessment and training; (2) feedback of trunk lean angles during walking to lessen loads on painful joints; and (3) feedback of low back loads during a lifting task. Preliminary data collected during tests of these applications suggest that the use of the display conveys benefits to

motor learning. To evaluate these effects more completely, further research is needed to compare the use of volumetric displays to other forms of feedback commonly used to enhance motor learning.

TABLE OF CONTENTS

LIST OF FIGURES

LIST OF TABLES

ACKNOWLEDGEMENTS

I would like to acknowledge everyone who helped me during my project, starting with Dennis Ripka for constructing the two string displays based on my designs, and Nori Okita for teaching me how to use the motion capture system.

I would like to thank my roommates who gave up their time to participate as my test subjects. I would also like to thank the other graduate students in the Biomechanics lab who helped me during calibration, and gave me feedback on how the display looked.

I would like to especially thank Dr. Stephen Piazza, my advisor, for helping me throughout the entire process. Without him, I would not have had the guidance necessary to complete this endeavor. I hope that future students will be able to expand upon my work.

Lastly, I would like to thank my family for supporting me as I tried to complete this thesis. The dedicated work ethic that they have instilled was a great asset, and their positive push to keep striving for excellence was very much appreciated.

Chapter 1

Introduction

The study of biomechanics emerged as a science during the Renaissance, when Leonardo da Vinci, Galileo Galilei, and Giovanni Borelli developed the foundation of this discipline by studying how muscle forces produce movement (Baker, 2007; Guglielmelli et al., 2015). In the 19th century, the study of human movement was again revolutionized by Eadweard Muybridge, who used a series of still photographs to analyze how the body moves, taking into account the translations and rotations of the body segments (Muybridge, 1907). Later studies by Willhelm Braune and Otto Fischer utilized of a series of photographs taken in a dark room of subjects wearing lights placed over their joints (Baker, 2007). This method improved the accuracy compared to Muybridge because the same body location could be identified in each picture. The major drawback of these systems was that each frame was analyzed by hand, and it would take a great deal of time to complete the measurements and kinematic and kinetic calculations for even the shortest trial (Braune and Fischer took years to analyze just a few walking gait trials). With the advent of computers in the past 50 years, great strides have been made in motion capture and motion analysis. With multi-camera systems tracking many markers and force plates measuring ground reaction forces, position and force data are readily processed to obtain muscular joint moments. Additionally, identification of markers can be accomplished in real time, greatly reducing the time required for post processing data.

There have been very few applications, however, that make use of motion capture systems' real-time capabilities in order to provide feedback to the subject.

Hunt et al. used real time motion analysis to provide feedback of lateral trunk lean angle during walking with the goal of helping the subject reach a designated maximum angle (Hunt, 2013). Increasing the lateral trunk lean decreased the adduction moment at the hip and knee by reducing the distance between the center of mass of the trunk and the joint to provide pain relief for subjects with osteoarthritic joints. In this study, however, patients were not given visual feedback depicting their bodies but rather were shown an indication of the degree of trunk lean.

Another gait study using real time feedback was performed by Malone and Bastian. They explored the effects of distraction and conscious correction by studying subjects walking on a split-belt treadmill while the belts were set to different speeds, and measuring their step lengths (Malone and Bastian, 2010). After the subjects had adapted to the belts that moved at different speeds, the two belts were set to move at the same speed and the authors measured the number of strides it took for the subjects to return to a normal step length. The feedback for the correction group was intermittent video showing the legs moving in real time, but the only view of their own legs presented to the subjects was a sagittal plane view.

Several studies have compared the effectiveness of different types of feedback on motor learning. McNair et al., for example, compared two types of feedback to determine

which was more effective at limiting the ground reaction force during landing (McNair et al., 2000). One experimental group received feedback in the form of verbal instruction on how to position their body during landing. A second group received auditory feedback in the form of a sound played during landing whose volume represented the ground reaction force. Visual feedback was not provided to subjects, and only the auditory group was given real time feedback during the landing. The authors found that both auditory and instructional feedback were significantly effective in reducing ground reaction forces during landing compared with a control group that received no feedback, but there was no significant difference between the two experimental groups.

Volumetric displays show virtual objects in three physical dimensions. They have been used mainly for artistic purposes, in the entertainment industry, and by hobbyists. Volumetric displays range from simple string or LED displays to highly complex holograms. The latter has been used in movies like *Star War*s, or in concerts to bring deceased artists, such as Tupac Shakur, back to life in front of thousands of amazed fans. Volumetric displays instill a sense of wonder when people can see a virtual object represented in three dimensions that is not possible with an image displayed on flat two-dimensional screen where an object can only appear three-dimensional. Some previous investigators have built volumetric displays and successfully displayed objects with a 360-degree viewing angle (Favalora et al., 2002; Jing et al., 2014; Langhans and Guill, 2003; Schubiger-Banz and Eberle, 2008). Reports on the use of these displays have always involved the playback of recorded motions or static images; to date, no published

papers have described volumetric display of the output of a motion capture system in real time.

Using volumetric displays to study their potential for modifying human movement would convey certain benefits. Motion measurement is important for researchers to understand how a subject is moving, and for the subject to monitor their own movement while learning a task. For example, the ability of subjects to see their movements in a volumetric space could help them to understand their changing body position while performing a task (Patel et al., 2006). The learning of novel motor tasks could be improved by presenting three dimensional movement feedback to the subject that either exaggerates or minimizes movement errors. Such augmentations to reality could help subjects to identify their errors more easily, or could prevent subjects who make large errors from becoming discouraged.

Combining real time motion analysis and volumetric displays is potentially useful for motor learning. With proper placement of markers on the body and accompanying measurement of external forces applied to the body, motion capture systems offer the ability to calculate the muscular moments generated at any joint. These muscular joint moments could be used as the basis for essential feedback that could help the subject learn to do a task in an optimal fashion that maximizes performance and avoids injury. The volumetric character of the display gives more information to the subject than would display of a numerical joint angle or even a two dimensional depiction of the body. Volumetric displays could be used for teaching skilled movements, such as those

performed by factory workers or a jumping jack, or they could have applications in rehabilitation, by helping patients to relearn movements following neurological injury.

The purposes of this thesis were (1) to develop a novel real time volumetric display for human movement; and (2) to create three applications for the new display in three motor learning scenarios. The work described in this thesis represents the first interface between a volumetric display and a marker-based motion capture system. It is hoped that this combination will provide an augmented view of reality and deliver biomechanical information not available from other forms of visual feedback, such as mirrors or two-dimensional video. Three applications were developed to show the capabilities of the system, but the information gathered suggests that the volumetric display could be used during future motor learning studies to provide feedback for a variety of other applications.

1.1 Specific Aims:

The specific aims of this thesis were as follows:

1. Build a volumetric display large enough and with sufficient resolution to show human motion;
2. Use the output of a motion capture system to update the volumetric display in real time; and
3. Develop and demonstrate three motor learning applications
    a. Real-time posture assessment and training;

b. Feedback of trunk lean angles during walking to lessen loads on painful joints; and
c. Feedback of low back loads during a lifting task.

1.2 Thesis Overview:

This thesis describes the design and construction of a volumetric display; the real time interfacing of the display with the motion capture system; and the creation three motor learning applications. Chapter 2 reviews past literature on types of feedback used during motor learning studies, the use of the real time capability in motion analysis, and human movement shown in volumetric displays. In Chapter 3, the creation of a functional volumetric display is described. Chapter 4 discusses how the real time capability was included, and how a multi-segment human body was displayed. The final methods chapter (Chapter 5) establishes the creation of the three applications. A concluding discussion of the thesis project is provided in Chapter 6.

Chapter 2

Literature Review

The general areas discussed in this literature review are 1) the use of feedback in studies of motor learning, 2) applications of real-time motion analysis, and 3) volumetric displays of human movement.

2.1 Use of Feedback in Motor Learning Studies

In this section, examples of each type of feedback used in past motor learning studies are cited to provide context for the approach used in this thesis project. For a more thorough review of feedback in motor learning, the reader is referred to the review written by Sigrist et al. (Sigrist et al., 2013).

2.1.1 Visual Feedback of Motion

2.1.1.1 Video Feedback

Many studies have used movements recorded by video cameras to give visual feedback during motor learning studies (Sigrist et al., 2013). For example, Malone and Bastian used video cameras to record sagittal-plane views to help subjects adapting their step lengths on a split-belt treadmill with the belts running at different speeds (Malone

and Bastian, 2010). In other studies, pre-recorded video has been used to show the target movement to subjects. This type of feedback has been used with subjects kicking a soccer ball who were shown a sagittal-plane view of the target movement (Horn et al., 2005), and with subjects learning tai chi positions who were shown a frontal-plane view of the target movement (Patel et al., 2006). In the tai chi study, Patel et al. found that using three dimensional visual feedback was more helpful than two dimensional video in learning new positions.

2.1.1.2 Feedback Showing a Computer-Generated Model on a Flat Screen

Computer-generated images of captured motion have also been used to provide visual feedback. The visual feedback has taken the form of a comparison of two images representing the subject movement and the target movement, or the subject's movement alone. Comparison between subject and target movements using a computer model has been performed with dancing (Aristidou et al., 2015), tai chi (Patel et al., 2006), and rowing (Sigrist et al., 2011). Aristidou et al. and Patel et al. displayed full body avatars of the subject and teacher while Sigrist et al. displayed two virtual oars representing subject and target movements in their study of rowing. Feedback was used to show the subject how their motion differed from the target motion, but these three-dimensional motions were displayed on a two dimensional screen. In studies where there was not a target movement, visual feedback of body position was shown to the subject. Roosink et al. and Lee et al., for example, used motion capture to create an avatar of the subject that was displayed on a screen (Lee et al., 2015; Roosink et al., 2015).

2.1.1.3 Direct Visual Feedback

Visual feedback of human motion is not limited to video representations and other displays of motion; it also includes viewing one's own body while performing a task. Researchers have attempted to gage the effectiveness of such direct visual motion feedback in motor learning studies. For example, a study investigating the role of feedback in the subject's ability to pour water from a kettle into a cup used direct visual motion feedback during trials to compare it with other forms of feedback, including auditory and haptic feedback (Portnoy et al., 2015). The authors found that by the last trial, subjects were able to perform the task with auditory feedback without a significant difference compared to haptic and visual feedback groups. Another study making use of direct visual feedback involved the gait retraining of female runners using a mirror (Willy and Davis, 2013). The direct visual feedback aided the runners in maintaining correct form shown by the decreases in hip adduction angles from before gait retraining.

2.1.2 Visual Feedback of Motion Variables

In some studies, motion variables are provided to subjects by displaying a graph or a numerical value to the subject, either instead of or in addition to motion feedback. Joint angles have been used as feedback to train motions involving different parts of the body. Researchers have measured angles related to lateral trunk lean (Hunt et al., 2011; Hunt, 2013), trunk flexion (Roosink et al., 2015), elbow and shoulder flexion (Brokaw et al., 2013), and hip adduction (Willy and Davis, 2013). In these studies, subjects were

shown a joint angle on a graph so that they could adjust their movements to match the desired joint angles. Some studies have a target angle that the subject is instructed to reach via highlighted zone on a graph (Figure 1) (Brokaw et al., 2013; Hunt et al., 2011; Hunt, 2013), or displaying a signal to the subject when the desired angle is reached (Roosink et al., 2015), while other studies have involved limiting of a joint angle (Willy and Davis, 2013). In addition to joint angles, the muscular joint moments exerted by the subject have been provided as feedback. For example, the maximal lumbar moments from forward bending, twisting, and side bending have been calculated and displayed in graphs so the subject could see how different lifting styles affected the values (Lavender et al., 2002).

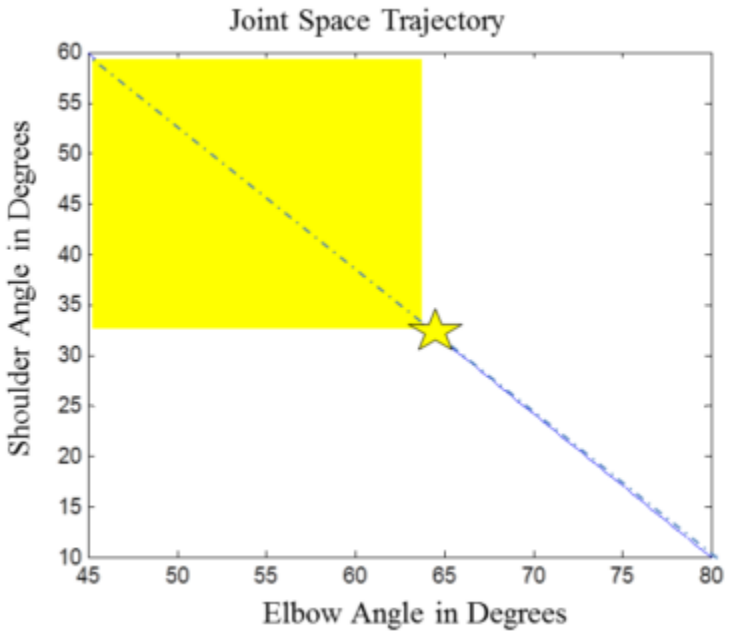

Figure 1: Example of visual feedback provided to subjects by Brokaw et al. (2013). The yellow area is the desired target for both shoulder angle and elbow angle, and the subject's current position is shown by a star. Subjects use this feedback to alter this movement to enter into the target range.

Other position variables have been used as feedback in motor learning studies. Krishnan et al. showed subjects the target ankle trajectory and their own trajectory on the same graph with the instructions to adjust their gait to match the template (Krishnan et al., 2015), while Kernodle and Carlton told subjects their throwing distance after each trial so subjects could adjust to attempt to throw further (Kernodle and Carlton, 1992). Sigrist et al. and Battini et al. gave feedback through color mapping data (Battini et al., 2014; Sigrist et al., 2011). Sigrist et al. used an arrow that changed size and direction for the distance away from the target, and changed the color of the arrow to indicate the rotation of the oar. Battini et al. scaled indications of ergonomic variables from green to red based on the OWAS, NIOSH, RULA, and OCRA values of warehouse workers during refilling, picking and packing (Battini et al., 2014). Kim et al. correlated subject position on a treadmill with the belt speed and gave feedback of target and actual speed to the subject on a screen (Figure 2) (Kim et al., 2015).

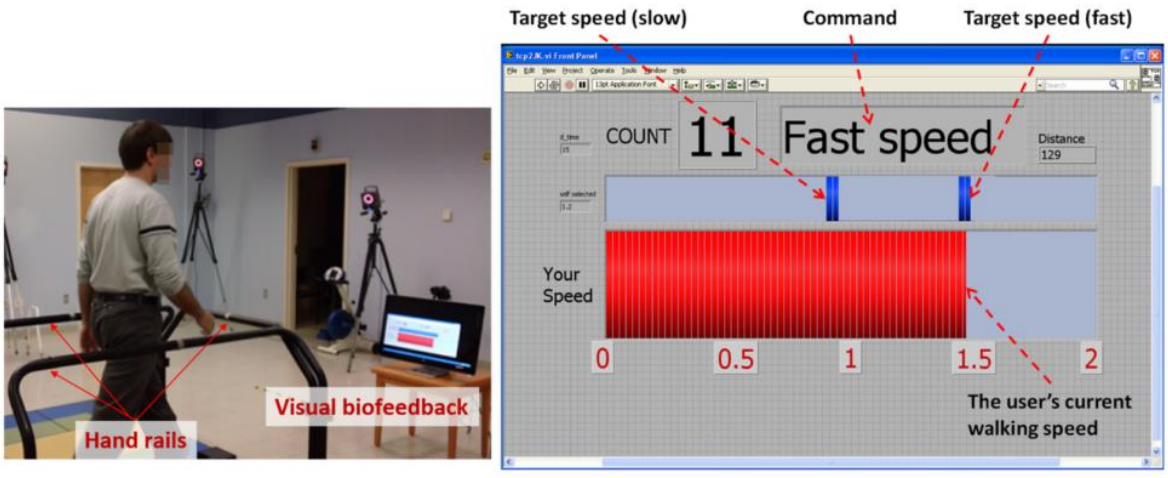

Figure 2: Experiments performed by Kim et al. (2015). Subjects were provided feedback on a screen that showed their current speed (red) and the target speed (blue).

2.1.3 Auditory Feedback of Motion Data

Auditory feedback representing motion variables has also been widely used in motor learning studies. Examples of motion variables used in such studies making use of auditory feedback are ground reaction force (McNair et al., 2000), lumbar moments (Kernozek et al., 2006; Lavender et al., 2002), position (Portnoy et al., 2015), and orientation (Sigrist et al., 2011). McNair et al. and Sigrist et al. used volume changes to indicate changes in ground reaction force and target position deviations, respectively. Kernozek et al., Lavender et al. and Sigrist et al. used pitch changes. Additionally, Sigrist et al. used changes in timbre, or the quality of sound, to help the user determine the correct rotation of the oar in a study of rowing. Portnoy et al. used a constant tone to inform the subject that the position of the kettle spout was over the cup in which they were pouring water.

2.1.4 Verbal Auditory Feedback

Auditory feedback has also taken the form of coaches providing feedback in the form of verbal instruction. Coaching was used to decrease the ground reaction forces of subjects landing (McNair et al., 2000), and the lumbar moments of subjects during lifting (Kernozek et al., 2006; Lavender et al., 2002). Coaching has also been used in studies to provide subjects with feedback on their movements in comparison to a target movement. Focus on particular indications of errors in movements have been given during many

different complex tasks: running (Willy and Davis, 2013), dancing (Gray et al., 2002), ball throwing (Kernodle and Carlton, 1992), and jumping (Sadowski et al., 2011).

2.1.5 Haptic Feedback

Haptic feedback includes both tactile (vibrations and pressures on the skin) and kinesthetic (involving muscle and tendon proprioceptors) (O'Malley and Gupta, 2008). There are many examples of the use of haptic feedback, including feedback through special gloves to analyze automotive designs (Bordegoni et al., 2006), estimate belly size in virtual environment (Normand et al., 2011), and aid subjects in pouring water into a cup while blindfolded (Portnoy et al., 2015). Although many simple tasks have found haptic feedback effective, Sigrist et al. stated that more studies on its effectiveness during complex tasks needed to be conducted because there have not been many studies supporting its use (Sigrist et al., 2013).

2.1.6 Immersive Three-Dimensional Visual Feedback

Some researchers have used "immersive" visual feedback that gives the subject the sensation of being in a three-dimensional virtual environment. Such studies are discussed in further detail in Section 2.3.1 Human movement along with other three-dimensional forms of motion feedback.

2.2 Real-Time Motion Analysis

While it is possible to provide feedback after the motion trial has concluded, many researchers have investigated motor learning effects using real-time feedback (Sigrist et al., 2013). Real-time feedback involves the calculation of specific motion variables as the motion is occurring that permit the subject to make adjustments during the trial. Electromyography (EMG) was used by Dolan et al. to estimate spinal compression in real time from the erector spinae during lifting (Dolan and Adams, 1998). Dolan et al. correlated EMG signals to the force the subject exerted on a load cell, and correction factors were used to adjust for changes in muscle length and contraction velocity. Motion tracking provides positions of specific points on the body that can be used to further calculate values like joint angles, joint moments, or animation of a model performing the movement. Three types of motion tracking used for feedback of human motion are wearable sensors, markerless motion capture, and marker-based motion capture.

2.2.1 Tracking of Body-Worn Sensors

Sensors worn on the body includes inertial measurement units (IMUs), measuring acceleration and rotations in three dimensions, potentiometers, measuring one-dimensional rotation at a joint, and electromagnetic sensors, which track three-dimensional sensor positions and orientations. IMUs placed on individual body segments have been used to calculate body position to create a computer-generated model of the

subject's body. Battini et al. and Lee et al. instrumented their subjects with multiple IMUs, and used the position data to create three-dimensional images of warehouse workers lifting that were updated at 500Hz (Battini et al., 2014), and soldiers in the battlefield that were updated at 30 Hz (Lee et al., 2015). In two case studies, Battini et al. reduced the risk of musculoskeletal injuries through ergonomic feedback and increased productivity, validating the proposed system. Lee et al. used the kinematic and kinetic motion data to create an avatar and change the avatar's surroundings. Potentiometers have been successfully used to provide real-time feedback of joint angles (Sigrist et al., 2011). While studying lumbar moments during lifting tasks, Lavender et al. and Kernozek et al. used electromagnetic sensors, such as Ascension Flock of Birds, to track how the different body segments were moving with respect to one another by measuring magnetic changes between the sensors and the magnetic transmitter at 100 Hz (Kernozek et al., 2006; Lavender et al., 2002). Kernozek et al. and Lavender et al. were able to alert the subjects of their lumbar moments during lifting since the data was processed in real-time. Electromagnetic sensors provide data similar to that available from motion capture systems that use markerless or marker-based motion tracking.

2.2.2 Markerless Motion Capture

Markerless systems, such as the Microsoft Kinect, are able to capture subject motion that can be used to calculate various motion variables. The Kinect uses an infrared projector and CMOS sensor to see a three dimensional environment (Zhang, 2012). Brokaw et al. used a Kinect interfaced with an algorithm to calculate subject

elbow and shoulder flexion during reaching (Brokaw et al., 2013). Kim et al. used a similar technology, Xtion, to determine the subject's position on an interactive treadmill to keep the subject in the middle of the treadmill by adjusting the belt speed (Kim et al., 2015).

2.2.3 Marker-based Motion Capture

Marker-based motion capture consists of multiple cameras that sample the capture volume at a high frequency, typically 100 Hz for human movement, and determine the three-dimensional coordinates of markers placed on a subject's body. Individual markers are typically placed at anatomical landmarks to create anatomical coordinate systems and cluster markers are placed in the middle of segments to represent the motion of the underlying bone. There are two types of markers that can be used: active markers that generate their own light using LEDs, and passive markers that are typically small spheres covered with reflective tape. Both types of markers have been used effectively in motion capture. For example, active markers have been used to capture subject motion from simple walking (Krishnan et al., 2015) to complex dancing (Aristidou et al., 2015).

Position data from the markers has been used to update virtual avatar positions (Kilteni et al., 2012; Normand et al., 2011), as well as to determine the three-dimensional position of the subject's body to determine range of motion (Kurillo et al., 2012) and body location and joint angles during pouring water (Portnoy et al., 2015). Similar to Portnoy et al., many other researchers have used passive marker motion capture to

compute real-time joint angles so subjects can adjust movements to reach target angles. For example, lateral trunk lean during gait (Hunt et al., 2011; Hunt, 2013) and trunk flexion while standing and sitting (Roosink et al., 2015) have been determined from marker data in real time.

2.3 Volumetric Representation of Movement

There is interest in visual three-dimensional movement feedback, which has been accomplished by head mounted stereo goggles during motor learning studies. There have been recent efforts to create volumetric displays, but none to date have been used to display human motion.

2.3.1 Human movement

Immersive three dimensional displays are used to give the subject visual feedback about a virtual environment. Kilteni et al. and Normand et al. each used head mounted stereo goggles to create a first-person virtual environment by displaying an image for each eye that accounts for binocular vision (Kilteni et al., 2012; Normand et al., 2011). Normand et al. used passive markers attached to a rod to control the belly size of an avatar to study how the subject's perception of their body could change when haptic feedback was removed. Kilteni et al. also used passive markers when creating the avatar in a virtual environment. Subjects in this study were able to see virtual arms that matched their actual arm movements during a series of reaching tasks.

2.3.2 Volumetric displays

Current literature describes both swept, a screen rotating about a midpoint with a changing image, and static volumetric displays, three dimensional images volumetrically (Langhans and Guill, 2003). A swept display design is described by Favalora et al. (Favalora et al., 2002), while static displays have been used in the form of a crystal prism with light projected into it (Jing et al., 2014; Langhans and Guill, 2003) and LED cubes (Figure 3) (Schubiger-Banz and Eberle, 2008).

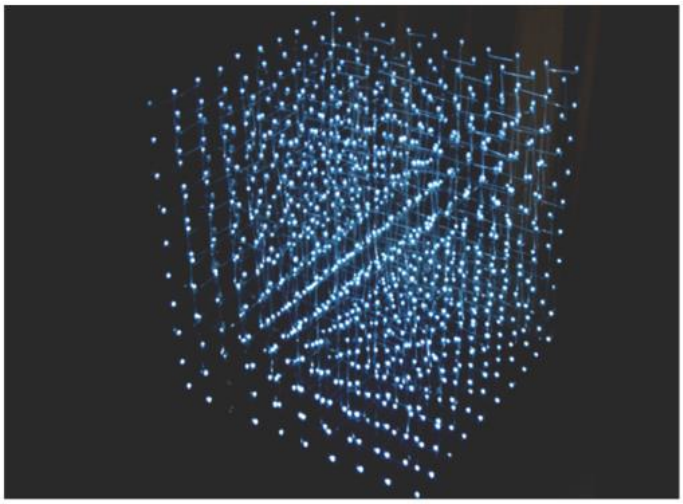

Figure 3: Volumetric 10 x 10 x 10 LED display (Schubiger-Banz and Eberle, 2008).

Another class of volumetric displays is string displays, which are paired with a projector (Figure 4). The string display works by projecting light onto an array of strings that would intersect the displayed object if it were placed in the display volume. By illuminating strings at various distances away from the projector, the image becomes volumetric. There are no published reports describing the use of a string display.

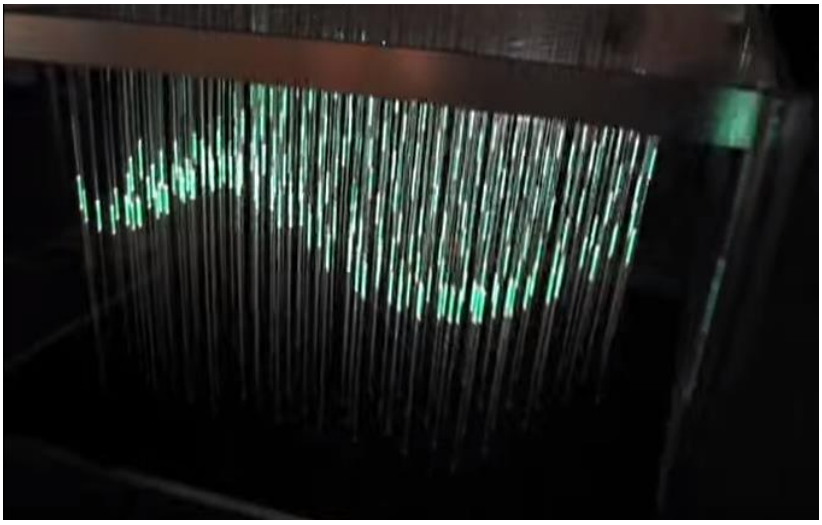

Figure 4: Volumetric string display (https://www.youtube.com/watch?v=pVFcSfUBWSk).

Chapter 3

Methods: Volumetric Displays

3.1 Physical Construction of Volumetric Displays

Three design iterations of volumetric displays were used in this study and each was calibrated to display images. The first design was a light-emitting diode (LED) Display, the second was a small string display, and the final design was a larger string display.

3.1.1 LED Display

The process of building a volumetric display began with the idea of using a three-dimensional array of LEDs. This decision was arrived at after viewing several YouTube videos showing that LED arrays could display human motion, although it could not be determined if these displays were driven by data collected using a motion capture system, and the videos certainly did not portray real-time displays. An LED cube with 4 LEDs on a side (4 x 4 x 4) was constructed from a kit (Jameco). The kit required soldering to construct the cube as well as the fabrication of a circuit board for the controlling circuitry that was built around a microcontroller. The display could be programmed by downloading a script from a PC to the microcontroller via a USB cable. A mapping was created to determine the link the coordinates of each of the LEDs to its indexing for the microcontroller.

There were some problems with using the LED cube to display human motion data collected using a motion analysis system. Doing so would have required replacing the script-based LED control with something different that would work in real time. Additionally, constructing an LED cube of the size necessary to display human motion (perhaps 64 x 64 x 64 or larger) would have involved considerable time and expense. For these reasons, alternatives to the LED cube were explored.

3.1.2 String Display

An attractive alternative to the LED cube was the string display that has been featured in art exhibitions. The string display operates by using a projector to illuminate an array of vertical strings to create a virtual representation of a three-dimensional object that is viewable from any angle around the display. The image projected by the projector is a series of rectangles, each of which falls upon an individual string in the string array to represent the intersection of the object with the strings (Figure 5).

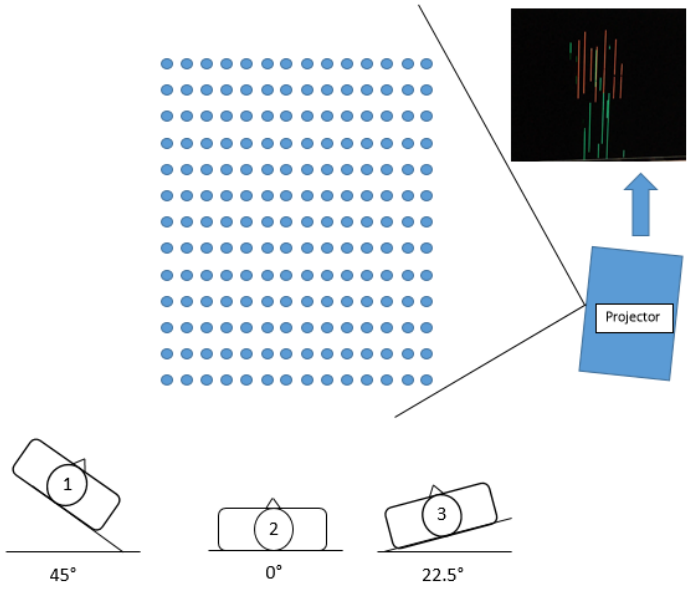

Figure 5: Schematic drawing showing an overhead view of three different observers (1-3) of the volumetric display. Observers 1 and 2 view the display at 45° and 0°, respectively, which are bad viewing angles because only a few strings may be viewed without obstruction by other strings. Such poor viewing angles are repeated at 45° increments around the display. Observer 3 has a better viewing angle that permits observation of more strings at once.

Proper placement of these rectangles requires a calibration that produces a mapping of the three-dimensional space onto the two-dimensional projected image. Although no published reports on the use of such a display could be found, the string display seemed well suited for use with a motion capture system. All that would be required would be to locate the object from the measured marker locations, determine intersections between the strings and the object, and use the intersection data to draw rectangles on the projected image (Figure 6).

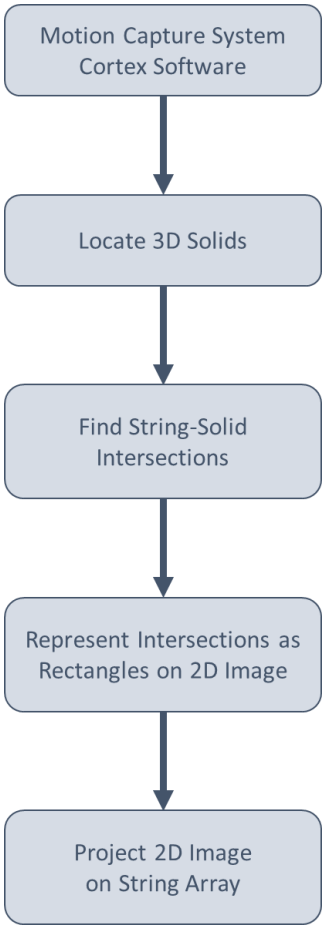

Figure 6: Overview of steps taken to display three-dimensional motions using the string display.

3.1.2.1 String Display: First Prototype

In contrast to the construction of the LED display, construction of the string display was less expensive and less labor intensive. A milling machine was used to drill ¼" holes in a 7 x 7 grid into two 16" x 16" x ¼" plywood pieces that would become the top and bottom of the display (Figure 7). Four ¼" x 2" x 3' wood pieces serve as vertical supports connecting the top to the bottom. White cotton string, diameter = .75 mm, (Baroque; 100% crochet cotton) was passed through the top board and bottom board and a piece of white elastic string, diameter = 1 mm (Loops & Threads; round cord elastic)

connected in series with each string kept it under tension. The front left leg could be removed to prevent it from casting a shadow on the strings (Figure 8).

Figure 7: Small string display with leg.

Figure 8: Small string display without leg.

3.1.2.2 String Display: Second Iteration

A larger display was constructed so that larger and more complex images, including those of human motion, could be displayed (Figure 9). The top and bottom of the display were again made of plywood but were larger in this design, 48”x48”. An evenly-spaced 21 x 21 grid of ¼” diameter holes were drilled into the top and bottom with a spacing of 5 cm. The four legs of the display were made from two 2”x1” pieces of wood and are each 49” long. The exposed wood was spray painted with a flat black paint to reduce any reflection of the projected light. Corner braces were added to make the display more rigid and thus keep the strings oriented vertically. The second iteration was used with a 13x14 array of strings that filled out only 41% of the display because it was found that the full array of strings would cause some strings to be occluded by others. Strings were again kept under tension using pieces of elastic string.

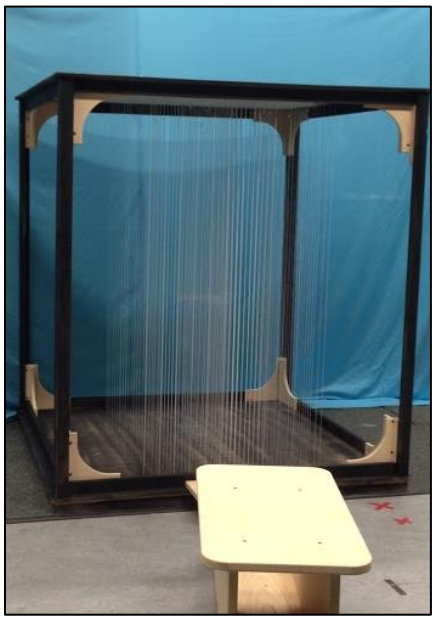

Figure 9: Large string display

3.1.3 Calibration

A calibration procedure was devised to find a mapping of three dimensional space onto a two dimensional projected image, and thus allow images of three-dimensional objects to be projected on to the strings properly. The calibration procedure yielded the rectangle parameters (horizontal position, vertical position, width, and maximum height) of each string, along with a scaling factor to account for the string's distance from the projector. The calibration was performed by positioning a green rectangle on a black background in a MATLAB figure (Figure 10) such that the projector (NEC VT676) illuminated the single string of interest (Figure 11). This was repeated once for each string in the display (i.e., 182 times for the large string display).

The calibration process began by selecting the string that was being calibrated. This was done by going sequentially through an entire row of strings and then moving to the next row. The position and width were then adjusted to illuminate only the desired string. The calibration process is illustrated in the form of a flowchart (Figure 12). To make the dimensions of the display uniform (i.e., to give the display a horizontal "ceiling" and "floor"), the same rectangle 300 units tall in the 400 x 300 MATLAB image (extending from the top of the image to the bottom) was projected on each string. The length of the illuminated portion of the string closest to the projector (h_1) was noted. The lengths of the illuminated portions of strings at the two corners furthest from the projector were noted as well (h_2 and h_3), and these three lengths were used along with the corresponding x- and z-locations of the three strings to develop the equation of a plane that could be used to predict values of h_i for each string in the display.

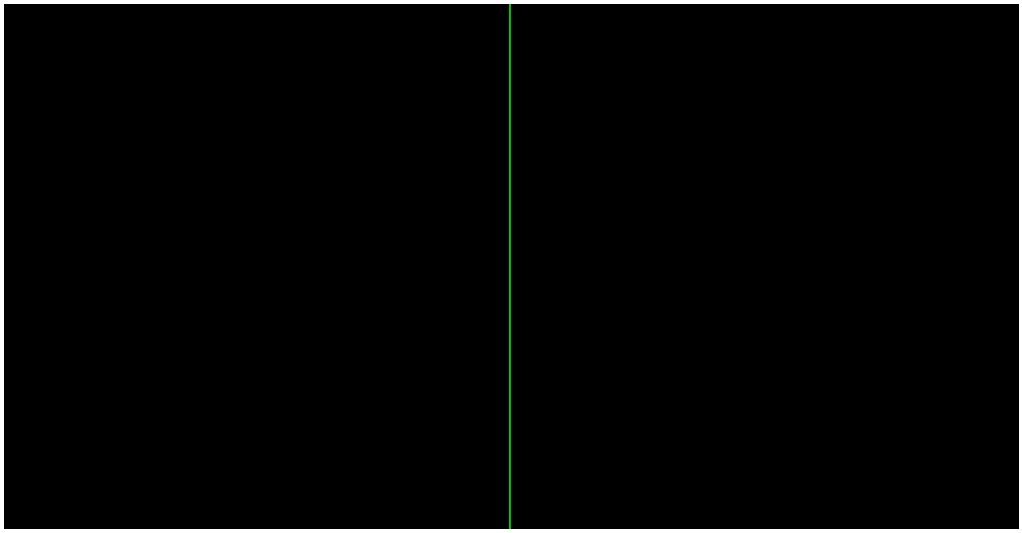

Figure 10: MATLAB image of calibration rectangle.

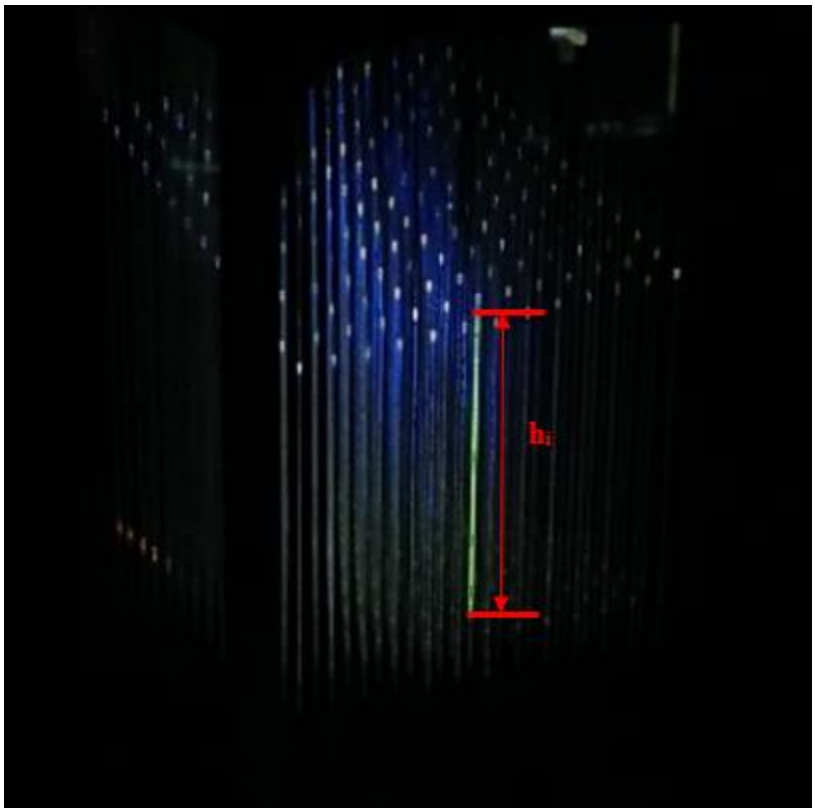

Figure 11: Calibration rectangle displayed on a string, with label for the viewable length of the string.

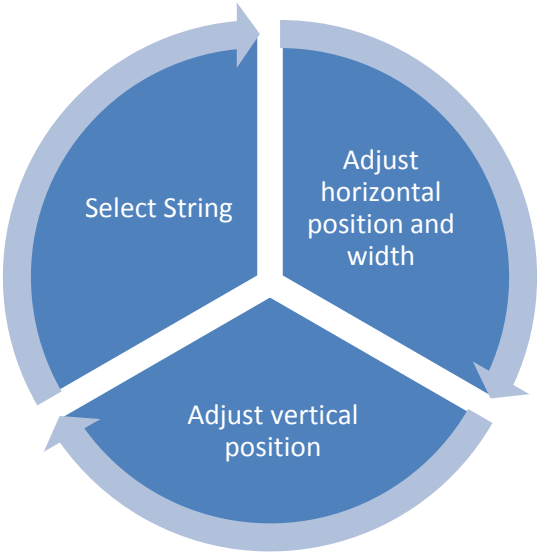

Figure 12: Flow chart of calibration process.

Following calibration, the x-position (x_i) and y-position (y_i) of the calibration rectangle in the image frame for each string were known, along with the width of the rectangle to be projected upon each string (w_i) and the height (h_i) corresponding to the length of string illuminated when the 300-unit rectangle was displayed upon it (Figure 13).

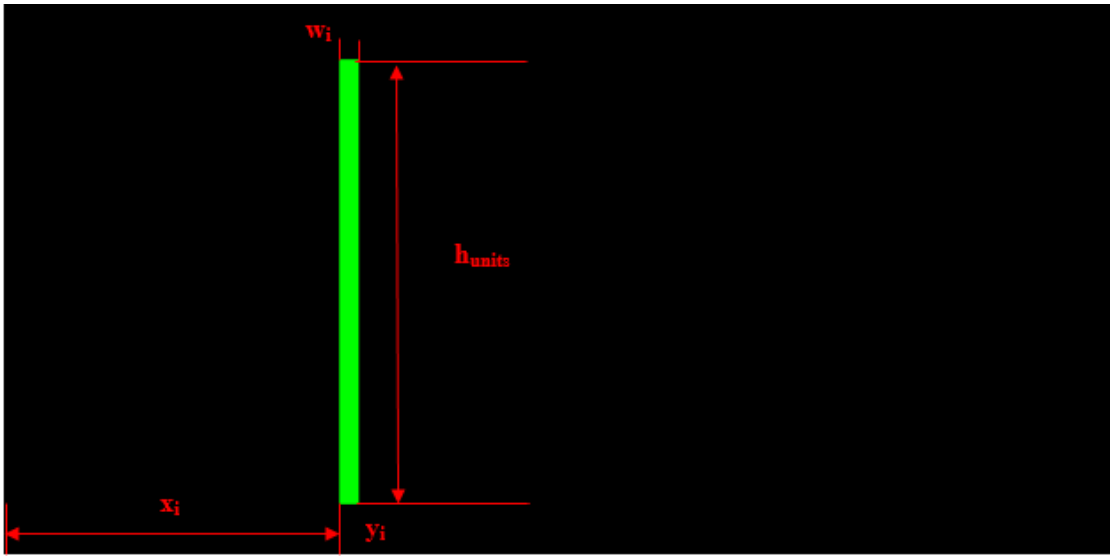

Figure 13: Measurements recorded from each calibration rectangle in the image reference frame.

All of these values were used when displaying objects using the intersections of the strings with the object to determine where in the MATLAB image the proper rectangles should be drawn. The illuminated height (h_i) was used to find a string specific scaling factor by dividing this value into the 300-unit height of the tallest rectangle. This scale factor corrected for the vertical spread of light from the projector and allowed strings further away from the projector to be illuminated with the proper height.

Once the calibration is complete, the X (X_g) and Z (Z_g) string locations in the global coordinate system were calculated using the number of strings and the distance between them. X_g and Z_g are the two directional vectors along the floor of the gait lab, Y_g is aligned with the vertical (Figure 14).

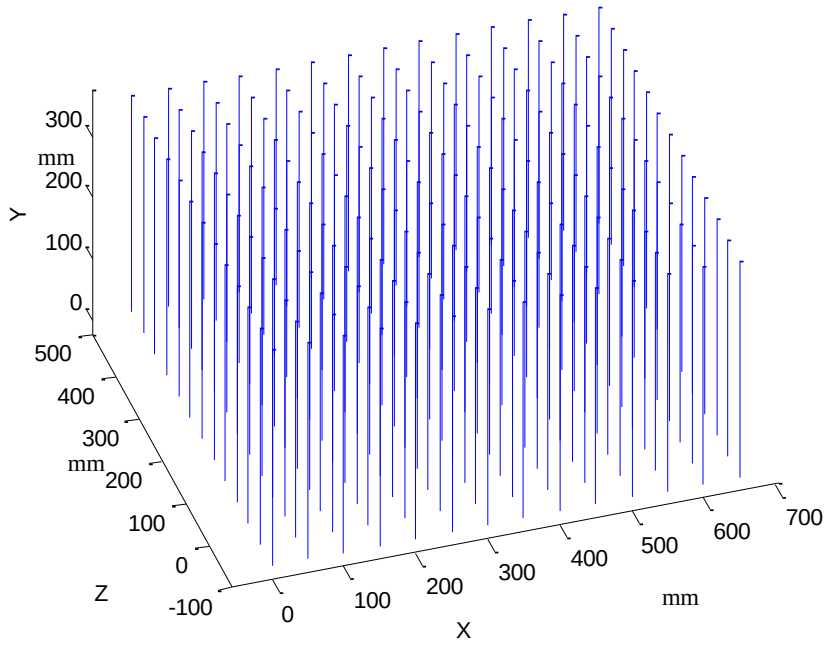

Figure 14: Layout of strings in the global coordinate system. Axes are in millimeters.

The calibration procedure is time consuming, but need only be performed once. To reproduce a given calibration after the projector or display has been moved, all that is needed is to display the calibration rectangles for each of the four strings in the corners of the array. The projector position is then adjusted until these strings display properly, at which point the calibration will have been restored.

3.1.4 String-Object Intersections

A six-camera motion capture system (Eagle; Motion Analysis Corp.) was used to track the three-dimensional locations of markers placed on objects to be shown in the volumetric display at 100 Hz. Intersections of the strings with these objects are then computed and used to illuminate the strings.

For the preliminary proof of concept, movement of a "dumbbell" was simulated by defining two spheres with a cylinder connecting them, and then rotating and simultaneously elevating the dumbbell. Each sphere was defined by a center point and a radius, and the cylinder was defined by two endpoints (the center points of the spheres) and a radius. Intersections between these objects and the strings were found using MATLAB routines for computing intersections between three-dimensional lines and either cylinders or spheres (Figure 15) (David Legland 2007).

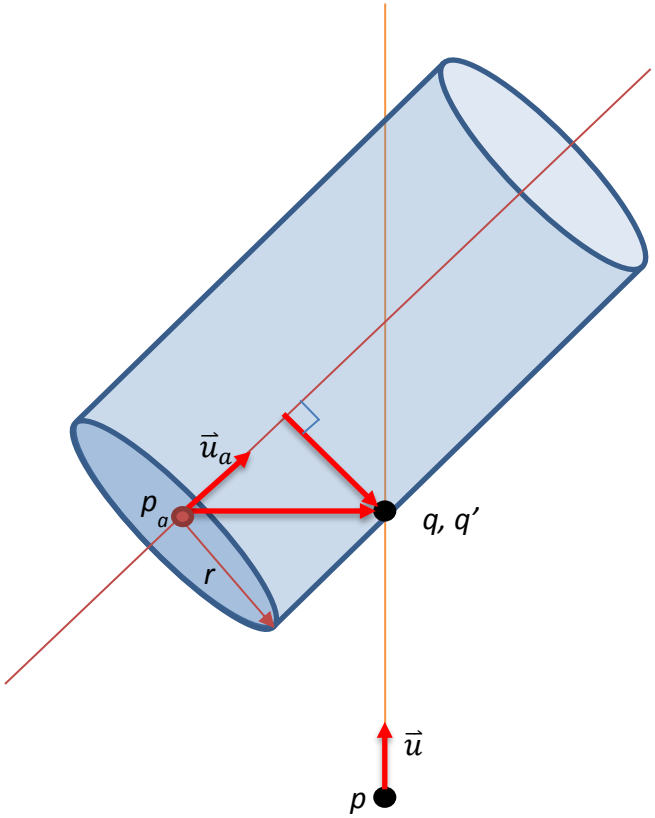

Figure 15: Intersection of a line (defined by point p and vector u) and a cylinder. The intersection is solved for by finding the roots of a quadratic equation in terms of the distance s from p along u.

The intersections between the strings and the cylinders were determined by first defining a point *q* on the surface of a cylinder of radius *r*:

$$|q - p_a - \vec{u}_a \cdot (q - p_a)\vec{u}_a| - r^2 = 0 \quad (3.1)$$

where p_a is a point on the cylinder axis and $\vec{u}_a$ is the unit vector along the cylinder axis. A point *q'* on a ray representing the string was defined by

$$q' = p + \vec{u}s \quad (3.2)$$

where p is a point on the ray, $\vec{u}$ is the unit vector of the ray, and *s* is the distance along $\vec{u}$ from *p* to *q'*. Setting *q* = *q'* by substituting (3.2) into (3.1) yields a quadratic equation in *s*. Solving this quadratic for *s* gives the point(s) of intersection between the ray and the cylinder. Finally, intersections between the string ray and planes representing the end caps are determined. A similar scheme was used to find intersections between strings and spherical objects, but in this case the point on the sphere was represented by:

$$(q - c)^2 - r^2 = 0 \quad (3.3)$$

where *c* is the center point of the sphere, and *r* is the radius of the sphere.

3.1.5 Display

A MATLAB figure with color and axis properties that matched those of the calibration figure was used to display the intersections. Matching of these properties was necessary so the calibration data (x_i, y_i, w_i and h_i) for each string would permit projection of light onto that string alone.

The display sequence used the intersections that were previously found, and the height of each of the rectangles was computed by subtracting the top and bottom intersection values for each string. These heights in millimeters are then transformed into height in image units by multiplying the values by the conversion factor determined from calibration, Eq. (3.4),

$$h_{rect} = \left|\frac{300}{h_i} * \Delta t_y\right| \tag{3.4}$$

where h_{rect} is the adjusted height of the intersection rectangle, h_i is the height of the calibration rectangle in millimeters, and Δt_y is the difference between intersection points for a particular string. The minimum height of a rectangle that can be displayed is one unit. If the height found is less than one unit, or if no intersection is found, the rectangle for that string-solid combination is set to display with a height of zero, making it invisible. A flow chart explains the display process (Figure 16).

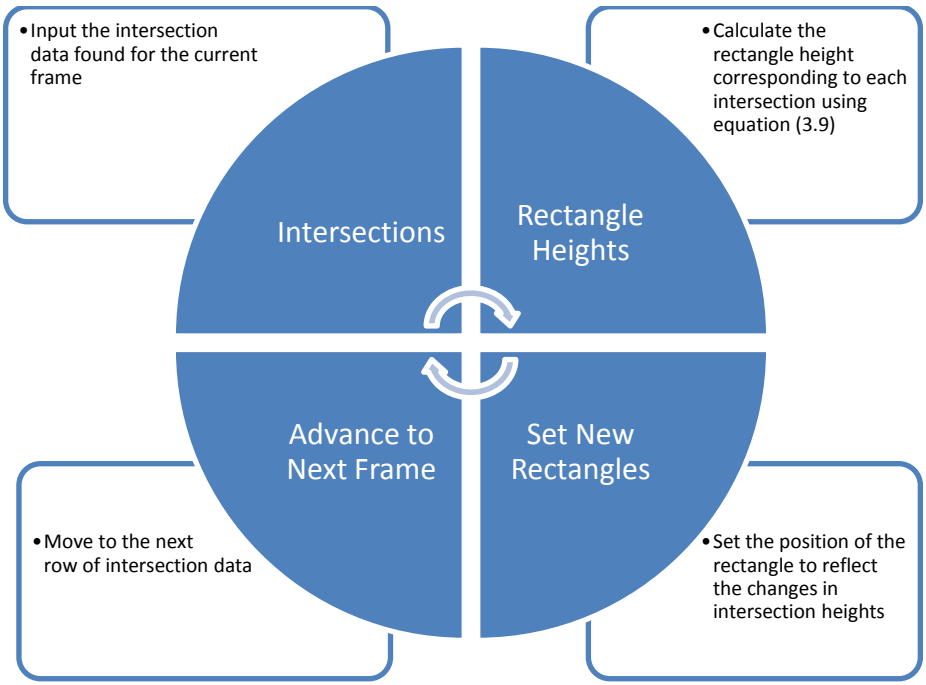

Figure 16: Flow chart illustrating intersection finding and display of rectangles.

3.1.6 Additional Simulations

Two further simulations were created to test the functionality of the display. The first was a simulated bouncing ball (Figure 17), and the second was a real bouncing ball that was captured by the motion system (Figure 18). The intersections of the first ball were calculated and displayed on the strings as in the dumbbell simulation.

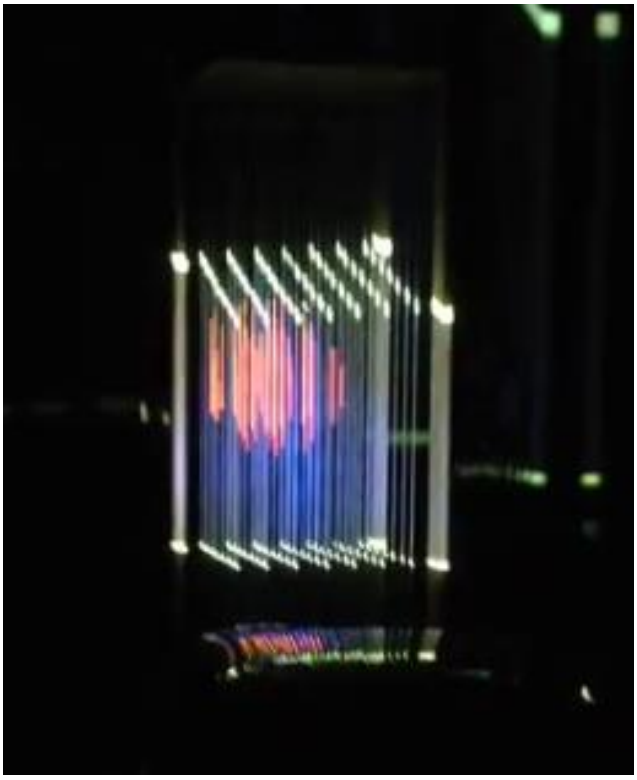

Figure 17: Image of simulated bouncing ball with coloring assigned according to the ball's velocity.

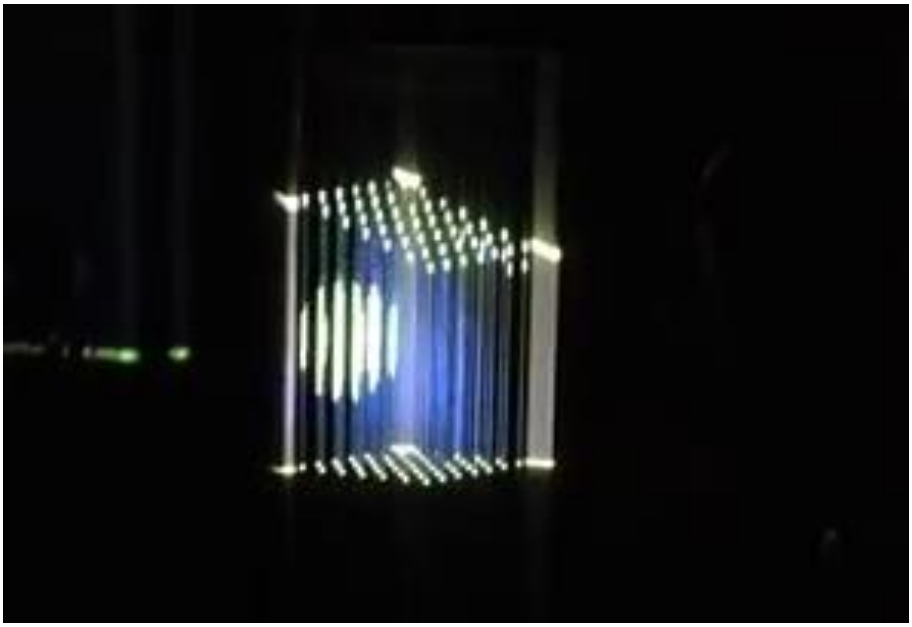

Figure 18: Image of real bouncing ball whose position was measured using the motion system.

The second ball was the first attempt at gathering coordinate data using the motion system. Five markers were attached to a soccer ball, and the soccer ball was dropped and allowed to bounce. The coordinate data were saved in the motion analysis system, and later exported and processed for use with the volumetric display. The radius and center of the sphere representing the ball were found using equations (3.5) to (3.7), that fit the least squares sphere to the marker data. Equation (3.5) was solved for each marker coordinate to find *a*, *b*, *c*, and *d*,

$$x_i{}^2 + y_i{}^2 + z_i{}^2 + a * x_i + b * y_i + c * z_i + d = 0 \qquad (3.5)$$

$$r = \sqrt{\frac{a^2+b^2+c^2}{4-d}} \qquad (3.6)$$

$$\vec{p}_{ctr} = \left[-\frac{a}{2} \quad -\frac{b}{2} \quad -\frac{c}{2}\right] \qquad (3.7)$$

where x is the x-coordinates of the points, y is the y-coordinates of the points, z is the z-coordinates of the points, *a*, *b*, *c*, and *d* are coefficients, r is the sphere radius, and $\vec{\mathrm{p}}_{\mathrm{ctr}}$ is the center point of the sphere.

The intersections between the strings and the sphere were calculated frame by frame, and the ball was projected onto the strings frame by frame. To demonstrate the capability of the display to portray information in addition to motion, the color of the simulated ball trial was changed to show the speed of the ball as it bounced.

These preliminary trials laid the groundwork to move forward with the larger display described in Section 3.1.2.2 String Display: Second Iteration. In addition, the tracking and display of the bouncing ball formed a basis for the display of motion data in real time.

Chapter 4

Methods: Real-time Display of Multi-Segment Human Bodies

After the volumetric string display was used to display the motion of a sphere, the next step was to represent motions of the human body in real-time. This chapter explores how the real-time capability of the motion system was exploited, and how the body of a human subject fitted with markers was represented by a collection of cylindrical segments.

4.1 Collection of Motion Data in Real Time

To make use of the real-time capability of the motion capture system, the marker coordinates needed to be continuously updated so that new intersections could be calculated and new rectangles could be displayed. The manufacturer of the motion system in the Penn State Biomechanics Laboratory (Motion Analysis Corp.) had previously developed a library that permitted these coordinates and other data in their Cortex software to become available in MATLAB in real-time.

When a large number of markers is being tracked, it is common for the system to lose markers briefly (or see them "drop out"). For this reason, error checking was added to the MATLAB routines so that when a marker dropped out it the body segment to which it was attached would not be displayed.

4.2 Representation of a Multi-Segment Human Body

4.2.1 Anatomical Coordinate Systems

The body was represented using ten cylindrical segments: right and left upper arm and forearm, right and left thigh and shank, pelvis and torso (Figure 19). The feet, hands and head were not included because the display is intended to show full body movements, and the resolution of the display would not be able to display the finer motions made by these body parts.

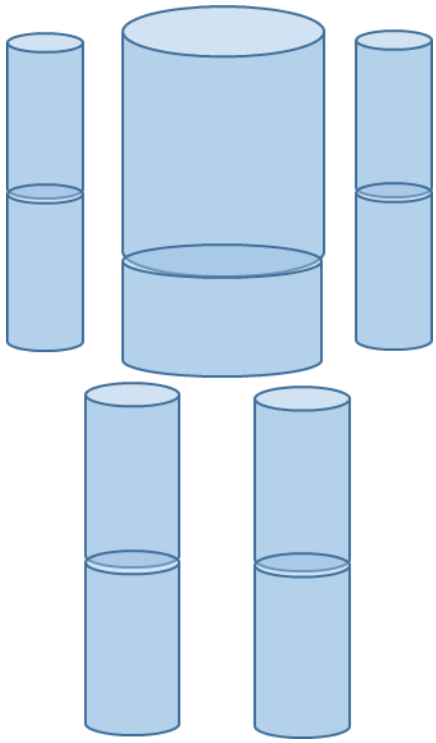

Figure 19: The human body was represented by ten cylindrical segments: (2) forearms, (2) upper arms, (2) thighs, (2) shanks, (1) pelvis, and (1) torso.

Prior to the motion trial, a static trial was performed in order to collect the locations of markers used to establish anatomically-aligned coordinate systems attached to each body segment. Subjects were instructed to stand in the middle of the capture volume with arms extended laterally, and feet shoulder width apart. For this static trial, sixty-three markers were symmetrically placed on the body (Figure 20; Figure 21). Markers were attached using double sided tape. Marker locations were:

- Left and right medial wrist, lateral wrist,
- Left and right medial elbow, lateral elbow,
- Left and right acromion-clavicular joint,
- Left and right medial malleolus, lateral malleolus,
- Left and right medial epicondyle of the femur, lateral epicondyle of the femur,
- Left and right greater trochanter,
- Left and right anterior superior iliac spine, posterior superior iliac spine,
- Sternum, vertebrae C7, and vertebrae T10.
- Clusters: Forearm, upper arm, thigh, shank, and pelvis.

For the dynamic motion trial, it was not necessary to track markers placed on anatomical bony landmarks. Instead, the motions of marker clusters were tracked. The reduction of markers allowed the subject to perform the tasks without the risk of knocking a marker off. These marker clusters were sets of four markers mounted on rigid curved plastic plates affixed to each body segment using toupee tape. For the torso

cluster, which was too large to track with a single cluster, the sternum and vertebrae markers served as the cluster (Figure 22; Figure 23).

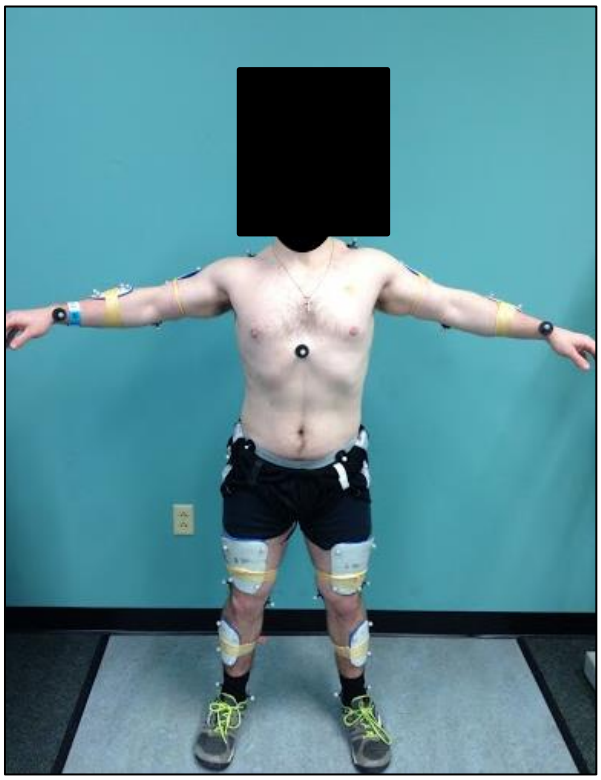

Figure 20: Anterior view of the marker set used in the static trial.

Figure 21: Posterior view of the marker set used in the static trial.

Figure 22: Anterior view of the marker set used in the dynamic motion trials.

Figure 23: Posterior view of the marker set used in the dynamic motion trial

The anatomical coordinate systems were defined using the static trial marker data, with marker locations expressed in the ground coordinate frame. Definition of a segment's anatomical coordinate system required specification of an origin and basis vectors for each body segment. The origin for each segment was centered at the proximal end of the segment (i.e. the forearm was centered in the elbow). These origins were found by averaging the coordinates of the markers at the proximal joint (e.g., the lateral and medial elbow markers), Eq. (4.1).

$$\vec{p}_{ctr_g} = \frac{\vec{p}_{lat_g} + \vec{p}_{med_g}}{2} \tag{4.1}$$

For the upper arm and thigh segments, the single marker on the shoulder and hip, respectively, was used as the origin. The pelvis and torso endpoints were computed differently from that of the limbs. The pelvis and torso had four markers at their intersection, but they were still averaged to find the center point to be used during the creation of both of their anatomical coordinate systems. Also averaged were the distal ends of the segments so that the long axis of the segment could be defined. The length of each segment was found by calculating the magnitude of the difference between the proximal coordinate and the distal coordinate, Eq. (4.2). The lengths were used when creating the cylinders.

$$\left\| \vec{l}_{seg_g} \right\| = \vec{p}_{distal_g} - \vec{p}_{proximal_g} \tag{4.2}$$

In equation (4.3), the y unit vector for each system was created by dividing the length of the segment by the magnitude of the length to ensure that it was a unit vector.

$$\vec{y}_{seg} = \frac{\vec{l}_{seg_g}}{\left\| \vec{l}_{seg_g} \right\|} \tag{4.3}$$

A quasi-z vector for each limb was created by subtracting the medial coordinate from the lateral coordinate at the elbow or knee, Eq. (4.4). The segments surrounding that joint used the same quasi-z vector when calculating the x and z unit vectors. The torso and pelvis used a quasi-z vector that pointed from the left shoulder to the right shoulder, Eq. (4.5).

$$\vec{q}_{seg_g} = \frac{\vec{p}_{lat_g} - \vec{p}_{med_g}}{\left\|\vec{p}_{lat_g} - \vec{p}_{med_g}\right\|} \tag{4.4}$$

$$\vec{q}_{seg_g} = \frac{\vec{p}_{r_g} - \vec{p}_{l_g}}{\left\|\vec{p}_{r_g} - \vec{p}_{l_g}\right\|} \tag{4.5}$$

A series of cross products were done to calculate the x and z unit vectors for each segment, Eq. (4.6) and Eq. (4.7). The x unit vector was divided by its magnitude to insure that it was a unit vector. The z unit vector was not divided by its magnitude because the x and y vectors were already confirmed to be unit vectors. An example segment with labeled anatomical coordinate axes is shown in Figure 24.

$$\vec{x}_{seg_g} = \frac{\vec{y}_{seg_g} \times \vec{q}_{seg_g}}{\left\|\vec{y}_{seg_g} \times \vec{q}_{seg_g}\right\|} \tag{4.6}$$

$$\vec{z}_{seg_g} = \vec{x}_{seg_g} \times \vec{y}_{seg_g} \tag{4.7}$$

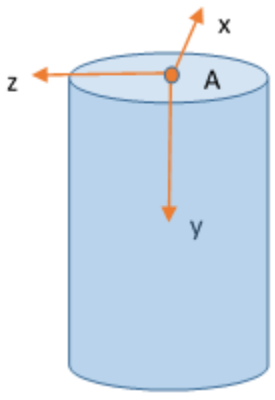

Figure 24: Example body segment with anatomical axes labeled

Using the unit vectors as the columns, a 3 x 3 rotation matrix, used to rotate reference frames about a series of angles, for each segment, Eq. (4.8), was formed and was then used to make the 4 x 4 transformation matrix between the ground frame cluster data to find the anatomical cluster data. The transformation matrix transformed the x, y, and z coordinates of a point in the anatomical reference frame into the global reference frame. The translation array, $\vec{p}_{ctr}$, was set as the origin for each segment in the global frame using equation (4.1) or the coordinate data for the shoulder and hip markers. The 4 x 4 homogeneous transformation matrix relating the anatomical coordinate system for each segment to the global coordinate system was found by combining the translation array with the 3 x 3 rotation matrix, Eq. (4.9).

$$R_{ga} = [\,\vec{x}_{seg} \quad \vec{y}_{seg} \quad \vec{z}_{seg}]_g \tag{4.8}$$

$$T_{ga} = \begin{bmatrix} & R_{ga} & & \vec{p}_{ctr} \\ 0 & 0 & 0 & 1 \end{bmatrix}_g \tag{4.9}$$

Using equation (4.10), the global cluster coordinate data was transformed into the anatomical coordinate system.

$$\vec{p}_a = {T_{ga}}^{-1}.\vec{p}_g \tag{4.10}$$

The cluster data in the anatomical reference frame is saved for each segment. These coordinates are assumed to be fixed because the cluster markers should not move with respect to the anatomical reference frame.

4.2.2 Definition of Cylinders for Body Segments

During a dynamic motion trial, the coordinates of cluster markers in the ground frame and the corresponding coordinates of the same markers in their respective anatomical frames were used to locate each segment in the ground reference frame. This was accomplished using the least squares method described by Challis (1995) that produced the 4 x 4 homogeneous transformation between coordinate systems that minimized the errors between markers. This transformation was then used to transform the coordinates defining the ends of the cylinder from the anatomical coordinate system to the ground coordinate system, as shown in Figure 25. Once transformed, these endpoints and generic segment radii, given in Table 1, were used to define the cylinders for the purpose of finding intersections as described in Section 3.1.4 String-Object Intersections. The values approximate measurements that would be expected for an average-sized male.

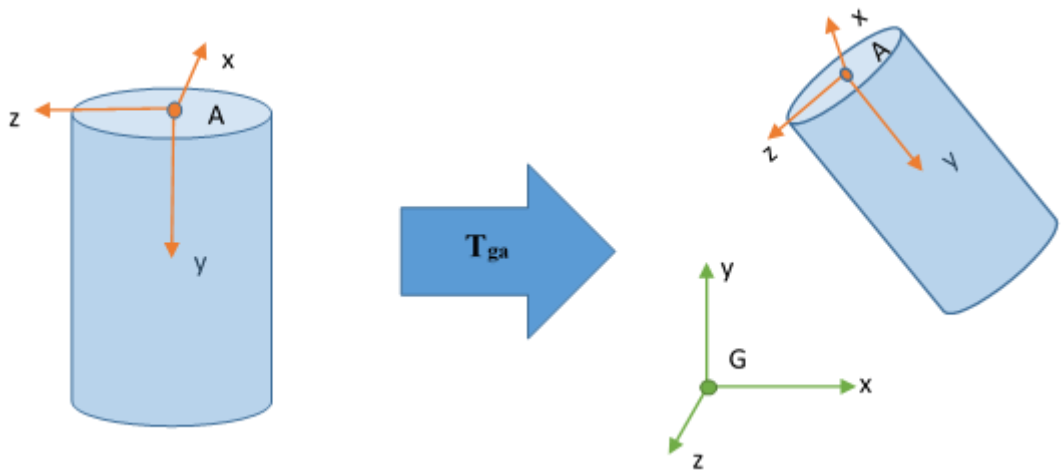

Figure 25: The transformation between the segment anatomical coordinate system A and the ground coordinate system G was used to locate a cylinder representing each segment in the ground coordinate system prior to finding string intersections.

Table 1: Generic Radii of Body Segments

Segment	Radius (mm)
Right Forearm	80
Right Upper Arm	80
Left Forearm	80
Left Upper Arm	80
Right Shank	100
Right Thigh	100
Left Shank	100
Left Thigh	100
Pelvis	160
Torso	180

4.2.3 Scaling

Location of the body segments was performed entirely within the full-scale ground coordinate system, but it was recognized that under some circumstances it would be useful to display a scaled-down (or scaled-up) version of the body in the display. To accomplish this, points defining the ends of each cylinder were multiplied by the desired scaling factor, as well as to the cylinder radii. For example, a scaling factor of 0.3 was used to display the whole-body motion of a subject 185 cm tall in the 30 cm tall display volume. To focus on different body parts, the coordinate data was adjusted until the desired intersections were seen on the display.

Chapter 5

Methods: Applications for Motor Learning Studies

Use of a volumetric display for real time representation of human movement was novel accomplishment but to demonstrate its utility, applications of the display for various purposes were developed. Three such applications were identified. Each was selected because it demonstrated the potential for usefulness in teaching a movement. The three applications were (1) real-time posture assessment and training; (2) feedback of trunk lean angles during walking to lessen loads on painful joints; and (3) feedback of low back loads during a lifting task. This chapter describes the three applications for the volumetric display and also presents expected results from a motor learning study that would be performed using each.

5.1 Real-Time Posture Assessment and Training

Control of balance and posture are factors thought to be of great importance to reducing fall risk and increasing stability in elderly populations (Lajoie, 2004). Feedback of postural sway has commonly been considered as a means for helping subjects to control their sway (Lajoie, 2004; Shumway-Cook et al., 1988; Swan et al., 2007), and the factors that influence postural sway (e.g., temperature, eyes open/closed) have likewise been the subject of much investigation (Mäkinen et al., 2005). The feedback presented in such studies has typically been in the form of a *stabilogram*, a two-dimensional plot showing the center of pressure as measured by the force plate upon which the subject

stands. In the proposed application, the volumetric display is used to provide feedback similar to a stabilogram but in three-dimensions.

For this application, the subject stood in the middle of the capture volume with feet shoulder width apart. The subject wore headgear fitted with markers (Figure 26), and the coordinates of these markers were collected and used to update the display in real time.

Figure 26: Headgear subjects wore during balance trials

The display showed the position of the subject's head as well as a target position, both of which were referenced to the center of the display. The subject and target positions were represented as discs with constant radii (r_{disc}) and heights (h_{disc}) of 100 mm and 50 mm, respectively. The subject would be instructed to match their position to

the changing target position. The target position is a function of an angle that increased a fixed amount each time the display updated. The target moved around the display volume in a circular path of radius R_{path}, as specified by Eq. (5.1) and Eq. (5.2). The vertical target position was set to fluctuate according to a sine function of the angle, Eq. (5.3).

$$x_{disc,t} = R_{path} * \cos(\theta) + 325 \tag{5.1}$$

$$z_{disc,t} = R_{path} * \sin(\theta) + 200 \tag{5.2}$$

$$y_{disc,t} = 100 * \sin(\theta) + 150 \tag{5.3}$$

The subject's motion was scaled to appear larger in the display, so that medial-lateral movement would span 0 to 600 mm, anterior-posterior movement would span 0 to 650 mm, and vertical movement, extending onto tiptoes or bending knees, would span 10 to 270 mm, Eq. (5.4) to Eq. (5.6).

$$x_{disc,s} = \frac{600}{175} x_g - 583 \tag{5.4}$$

$$z_{disc,s} = \frac{1}{2} z_g - 115 \tag{5.5}$$

$$y_{disc,s} = \frac{7}{4} y_g - 3245 \tag{5.6}$$

The distance between the centers of the discs (error, e) was calculated in real-time, Eq. (5.7), and determined the color of the target disc (blue e < 50 mm, red: e > 50 mm), (Figure 27; Figure 28).

$$e = \sqrt{(x_{disc,t} - x_{disc,s})^2 + (y_{disc,t} - y_{disc,s})^2 + (z_{disc,t} - z_{disc,s})^2} \quad (5.7)$$

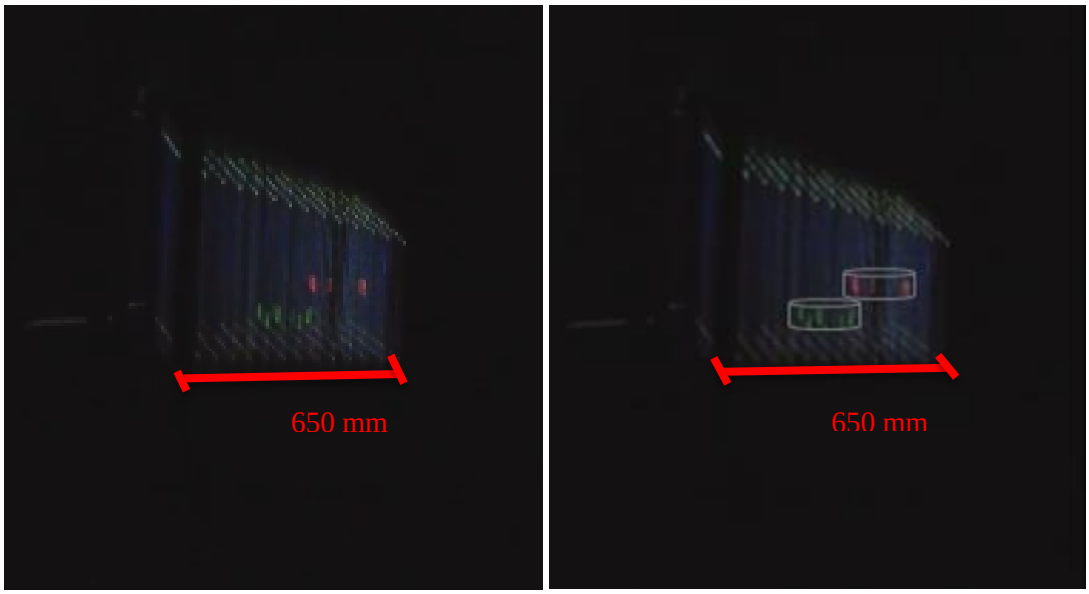

Figure 27: Subject (green) and target (red) discs moving through the display, error > 50 mm. The discs were outlined (right) to show the objects that were intersecting the strings.

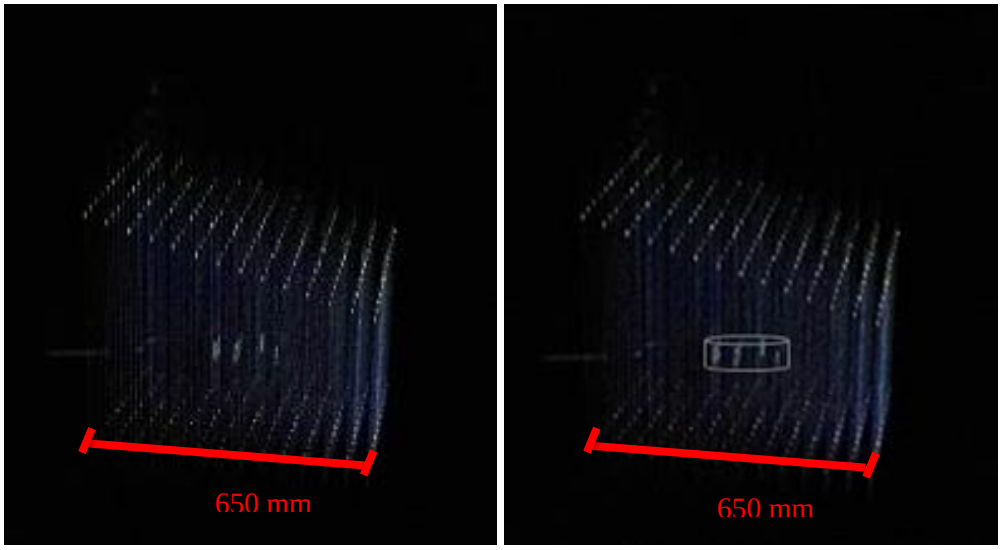

Figure 28: Subject and target disc are in same position, error < 50mm. Only a single disc is viewable because they perfectly overlap. The disc was outlined (right) to show the object that was intersecting the strings.

5.1.1 Expected Results

Expected results that would be expected from using this application in a balance training study are presented as a polar plot, with error *e* plotted as a function of angle (Figure 29). This polar plot would provide important information about which directions were most difficult for the subject to control his or her posture. This information would allow specific muscle groups to be targeted by strength training programs to improve the control of balance.

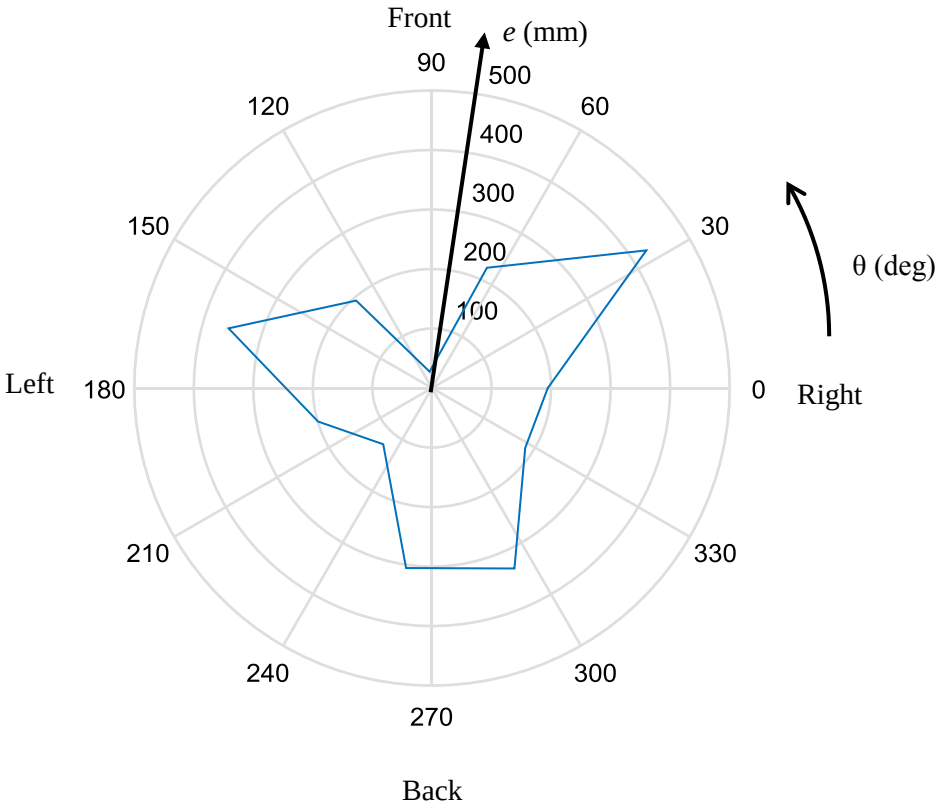

Figure 29: Expected results of balance study: angle of lean (θ) vs. average error (*e*) over the length of one trial.

5.2 Feedback of Lateral Trunk Lean during Gait

Hunt et al. studied how increasing the lateral trunk lean would reduce the knee adduction moment (Hunt et al., 2011). During gait, large joint moments are exerted by the muscles crossing the hip and knee of the stance leg in order to prevent these joints from collapsing in adduction. The gluteus medius muscle, for example, must produce large hip moments to counter the gravitational moment caused by the weight of the trunk. If the gluteus medius cannot produce a large enough moment, the pelvis will drop (known as Trendelenburg's sign). The force carried by gluteus medius also compresses the hip joint, which can contribute to hip pain in patients with degenerative hip osteoarthritis. Walking with an increased lateral trunk lean (over the stance-side hip) can reduce the demands on gluteus medius and thus may reduce hip pain (Hunt et al., 2011). Gait with a stance-side trunk lean is sometimes termed "antalgic gait" because of its role in limiting joint pain (Figure 30). This gait pattern is often adopted spontaneously by patients with hip osteoarthritis because they discover that it limits pain. Some patients, however, do not discover this gait on their own and could benefit from feedback to help them control their trunk lean in this way. By measuring and feeding back the angle of trunk lean subjects might find the ideal pain-relieving gait faster.

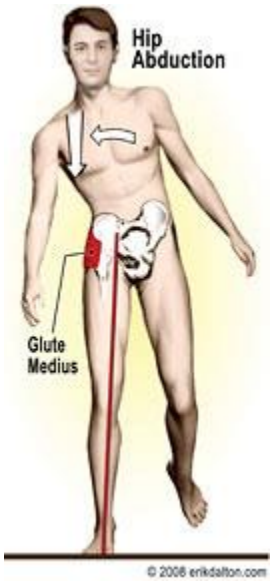

Figure 30: Illustration of "antalgic" gait in which there is a leaning of the trunk over the stance-side leg. This gait may be adopted to compensate for gluteus medius muscle weakness or to relieve pain in the knee or hip by reducing compressive muscle forces.

To demonstrate this application of the display, one healthy 22 year old subject was instructed to walk for two minutes with exaggerated trunk lean during right leg contact. The desired exaggerated trunk lean was set at 6º with a tolerance of ± 1º, which was based on the methods of Hunt et al.'s previous work. The desired moment arm upper bound was set at 127 mm. This trial was used to test the ability to calculate trunk lean real-time.

Computation of trunk lean angle relied on the kinematics processing techniques described in Chapter 4, followed by calculation of the trunk lean angle. To calculate the trunk lean, the rotation matrix between the torso and the ground was decomposed using a ZXY body fixed rotation, Eq. (5.13) to Eq. (5.16). This rotation sequence was chosen to avoid "gimbal lock" degenerate configurations, as the rotation about the X axis, pointing

posteriorly from the origin of the torso segment, would never equal 90 degrees. To make the coordinate axis better aligned with the ground coordinate system, the negative values of the x and y components were used. This change made x point anteriorly from the body, and y point up instead of down. Using trigonometry and a reference ZXY body fixed rotation matrix, Eq. (5.13), the three angles of rotation were found for each iteration of the code were saved.

$$Z_1X_2Y_3 = \begin{bmatrix} c_1c_3 - s_1s_2s_3 & -c_2s_1 & c_1s_3 + c_3s_1s_2 \\ c_3s_1 + c_1s_2s_3 & c_1c_2 & s_1s_3 - c_1c_3s_2 \\ -c_2s_3 & s_2 & c_2c_3 \end{bmatrix} \quad (5.13)$$

$$\theta_x = sin^{-1}(T_{ga}(3,2)) \quad (5.14)$$

$$\theta_y = tan^{-1}\left(-\frac{T_{ga}(3,1)}{T_{ga}(3,3)}\right) \quad (5.15)$$

$$\theta_z = tan^{-1}\left(-\frac{T_{ga}(2,1)}{T_{ga}(2,2)}\right) \quad (5.16)$$

Feedback was provided to the subject by changing the color of the display. The torso segment would change on a scale from white to red depending on the lateral trunk lean angle, θ_x, for that frame (Figure 31; Figure 32).

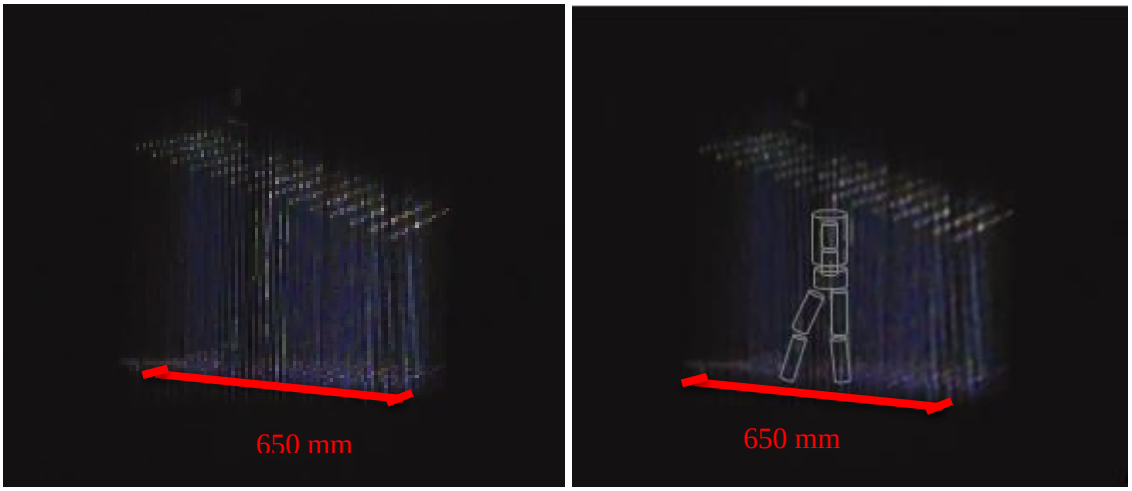

Figure 31: Subject image walking towards the left. Torso color (white) is determined by 5º< θ_x < 7º. The body segments were outlined (right) to show the objects that were intersecting the strings.

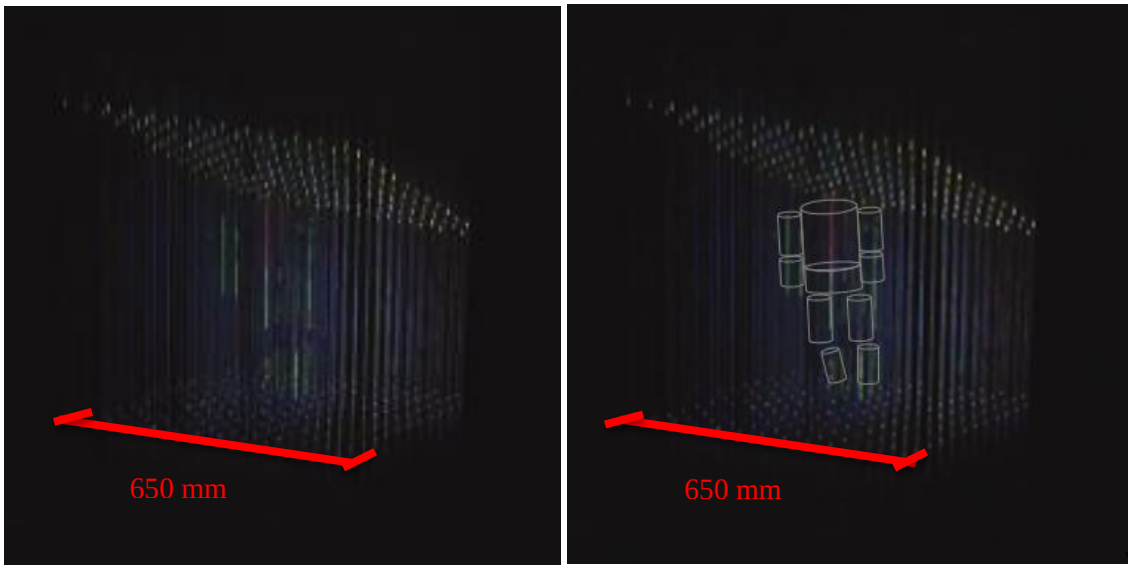

Figure 32: Subject image walking towards camera Torso color (red) is determined by 5º> θ_x or θ_x < 7º. The body segments were outlined (right) to show the objects that were intersecting the strings.

5.2.1 Expected Results

The expected results are displayed in test data that was collected is shown in Figure 33. The results show that over three sessions, the subject was able to get the average lateral trunk lean angle within the target range. The standard deviations of the angles also decreased from each of the first four sessions. A potential posttest outcome was displayed to illustrate how the average angle and standard deviation could show how well a subject learned the movement.

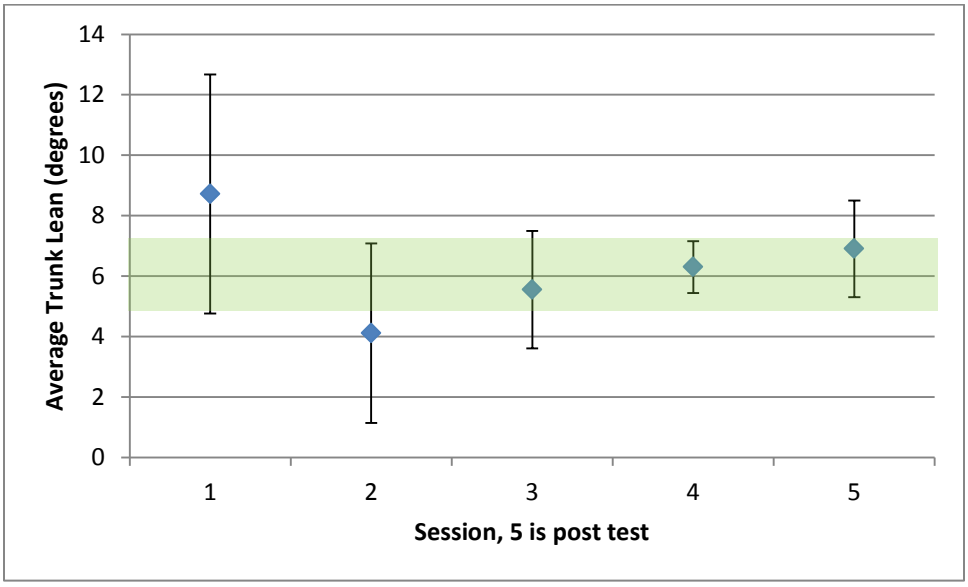

Figure 33: Expected results of gait study. Session 5 is the posttest assessment, a possible outcome shows that the subject maintains target lateral trunk lean. The green bar is the target zone for lateral trunk lean angle, 5º to 7º.

5.3 Feedback of Lumbar Moment Arm Length to Prevent Injury during Lifting

Lifting tasks can cause injuries to the back from large moments being generated during the lift (Manchikanti et al., 2014). Warehouse workers to everyday people performing lifts that are bending their backs, should be aware of how large lumbar moments can adversely affect them. Using this display, subjects would be able to see how changing the length in the moment arm can reduce the stress that is put on the lumbar joint.

For this application, the subject performed a series of twenty five lifts of a milk crate that had a 15.1 lb. weight in it (Figure 34). The weight was centered in the bottom of the crate, and was zip tied to the base so it would not move during the lifts.

Figure 34: Markers on the crate used for lifting

The lift combined both vertical and rotational movements, which are common in most daily lifting task (Kernozek et al., 2006; Lavender et al., 2002). From a relaxed standing position, the subject was tasked with moving the crate from the floor to a stool, 0.46 m high. The subject was never instructed how to lift, but was instructed to use the feedback from the display to position the body so the moment arm was less than 0.5 m for the duration of the lift. This application used the same process to find intersections and display the multi-segment body discussed in the Chapter 3 and 4, but additionally calculated the length of the moment arm in real-time.

The distance between the crate center of mass and the lumbar joint was calculated to give real time feedback of the moment arm. The same real time capability, anatomical coordinate systems, and cluster locations were used with the addition of four markers to define the crate (Figure 34). A crate specific coordinate system was created so that the center of mass of the crate with the attached mass could be found. The center of mass for the crate and weight were measured separately, and the combined center of mass was calculated, Eq. (5.1).

$$\vec{x}_{total_{crate}} = \left[\frac{(m_1\vec{x}_1+m_2\vec{x}_2)}{(m_1+m_2)}\right]_{crate} \tag{5.1}$$

Similar to the body segments, a transformation matrix from the ground coordinate system to the crate coordinate system was created. The origin for the crate was set marker 1, (Figure 35). To keep the y unit vector in the vertical plane, the x axis was determined by subtracting two markers coordinates, marker 1 and 2, Eq. (5.2). The quasi-z axis was

formed along the other edge of the crate by subtracting marker 1 from marker 4, Eq. (5.3).

$$\vec{x}_{crate} = \left[\frac{\vec{p}_2 - \vec{p}_1}{\|\vec{p}_2 - \vec{p}_1\|}\right]_{crate} \tag{5.2}$$

$$\overrightarrow{q_z}_{crate} = \left[\frac{\vec{p}_4 - \vec{p}_1}{\|\vec{p}_4 - \vec{p}_1\|}\right]_{crate} \tag{5.3}$$

A cross product between the quasi-z and x vectors determined the y axis, and a cross product between the x and y vectors determined the z axis, Eq. (5.4) and Eq. (5.5).

$$\vec{y}_{crate} = \frac{\vec{q}_{crate} \times \vec{x}_{crate}}{\|\vec{q}_{crate} \times \vec{x}_{crate}\|} \tag{5.4}$$

$$\vec{z}_{crate} = \vec{x}_{crate} \times \vec{y}_{crate} \tag{5.5}$$

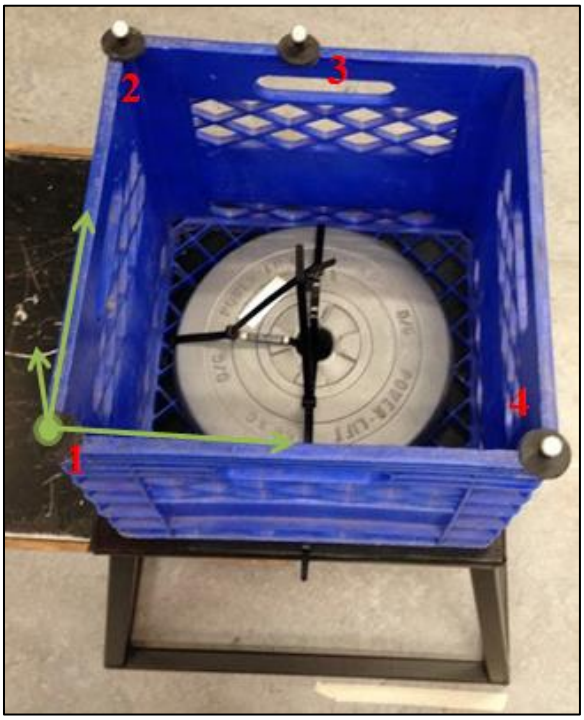

Figure 35: Crate specific coordinate axes

A rotation matrix and a translation array were again formed, Eq. (5.6). The translation array was the global coordinates of marker 1. The transformation matrix, Eq. (5.7), was used to convert the center of mass of the crate from crate coordinates to ground coordinates, Eq. (5.8).

$$R_{ga_{crate}} = [\,\vec{x} \quad \vec{y} \quad \vec{z}\,]_{crate} \tag{5.6}$$

$$T_{ga_{crate}} = \begin{bmatrix} \vec{x} & \vec{y} & \vec{z} & \vec{p}_1 \\ 0 & 0 & 0 & 1 \end{bmatrix}_{crate} \tag{5.7}$$

$$\vec{p}_g = T_{ga_{crate}} . \vec{p}_{a_{crate}} \tag{5.8}$$

To calculate the moment arm length, two vectors were created with origins at the center of mass of the crate, Eq. (5.9) and Eq. (5.10). The first vector, $\vec{v}_g$, pointed to the coordinate for the lumbar joint, which was set as the origin of the pelvis segment. The second vector, $\vec{u}_g$, was a negative y vector that represented the direction of gravity. The projection of the first vector onto the second vector was computed, Eq. (5.11), to find the point on the second vector that was closest to the lumbar joint. The distance between the closest point and the lumbar joint was the length of the moment arm, Eq. (5.12).

$$\vec{v}_g = [COM_{lumb} - COM_{crate}]_g \tag{5.9}$$

$$\vec{u}_g = \begin{bmatrix} 0 \\ -1 \\ 0 \end{bmatrix} \tag{5.10}$$

$$[proj_u v]_g = \left[\left(\frac{(\vec{v}\cdot\vec{u})}{\|\vec{u}\|^2}\right)\vec{u}\right]_g \tag{5.11}$$

$$d = \|COM_{lumb} - (COM_{crate} + proj_u v)\|_g \tag{5.12}$$

To provide feedback to the subject, the color of the torso was correlated to the length of the moment arm, *d*. The color varied on a scale from red to white based on the length of the moment arm (Figure 36; Figure 37).

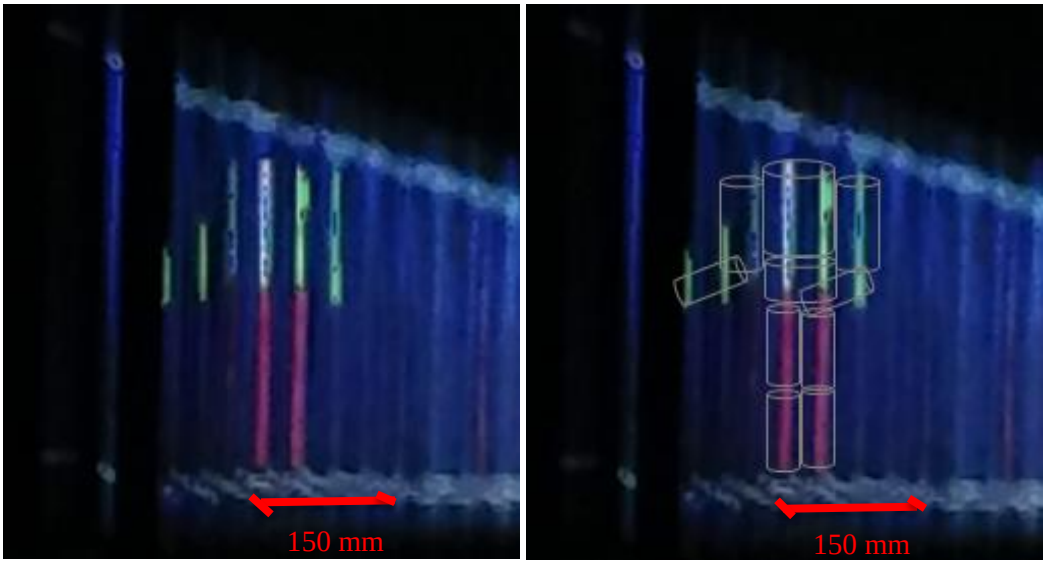

Figure 36: Subject standing upright, holding the crate, displayed with green arms, pink trunk (d > 300), red legs. The body segments were outlined (right) to show the objects that were intersecting the strings.

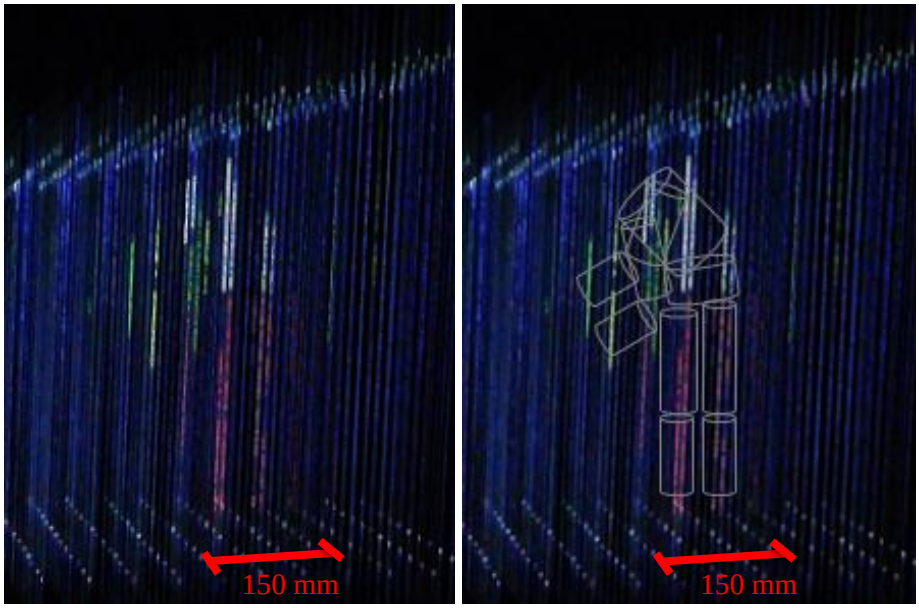

Figure 37: Subject bending to the left to place crate down, displayed with green arms, white trunk (d < 300), red legs. The body segments were outlined (right) to show the objects that were intersecting the strings.

5.3.1 Expected Results

The expected results are displayed in test data that was collected is shown in Figure 38. The results would give important feedback about the effectiveness of the display in a motor learning study of a similar lifting task.

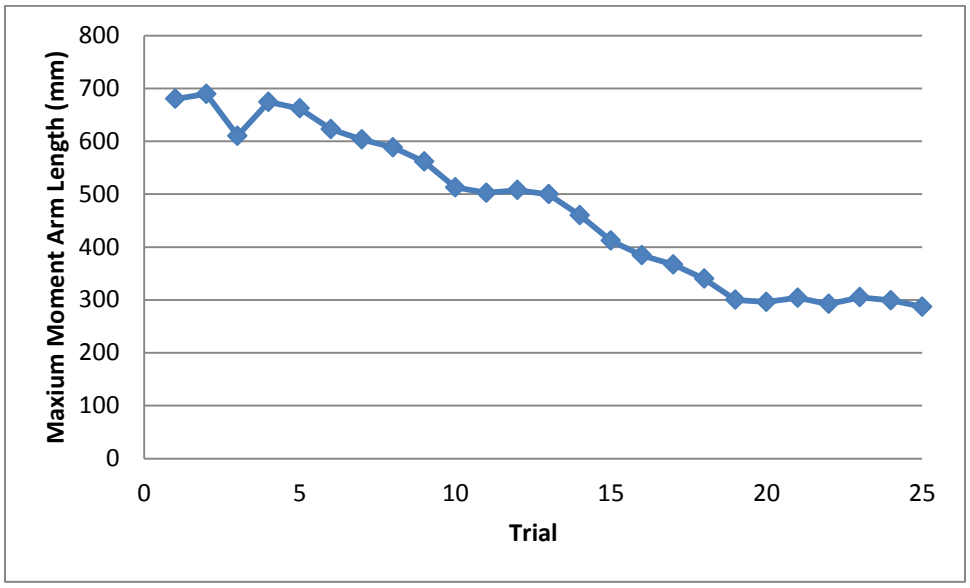

Figure 38: Expected results of lifting study: maximum moment arm length (mm) vs. trial.

5.4 Performance of Display

The data were captured at 100 Hz during each of the applications. During the disc application, a refresh rate of 12 Hz was observed. During the gait and lifting applications, a refresh rate of 8 Hz was observed. These rates were below the threshold for human vision, 18-20 Hz, so changes between frames could be seen. From time profiling the program, it was found that calculating the intersections between each solid and the strings took approximately 90% of the total time.

Chapter 6

Discussion and Future Directions

The work described in this thesis is the first example of a motion capture system used to display human motion in a volumetric display in real-time. There were three specific aims proposed:

1) ***Build a volumetric display***

After initially exploring (and constructing) a three-dimensional array of light-emitting diodes (LED cube) for the display, on the basis of cost, resolution, and ease of construction, it was decided to move to a display that projected light onto an array of strings. Two versions of such a string array were constructed: an initial smaller version followed by a larger version better able to display human movement. A calibration scheme was developed to enable mapping of three-dimensional positions of objects into a two-dimensional image projected onto the display. Both string displays were successfully used to display simulated motions of primitive solids (spheres and cylinders).

2) ***Display motions collected in real time using the display***

A video-based motion capture system was used to record the motions of objects and human bodies and those data were imported in real time into MATLAB routines that used the calibration-derived parameters to represent the motions properly in the display. The three-dimensional motions of primitive solids (a ball

bouncing) and humans (a subject performing calisthenics) were successfully displayed in real-time.

3) ***Develop three applications to show potential for use of the display in motor learning studies***

While conducting a full motor learning study was outside the scope of this work, three example applications were created to demonstrate how the display might be used in such studies. For each, a protocol was developed for motion capture and display of errors using different means for representing movement errors. Expected results were presented to give the reader an idea of the role motion feedback might play in improving motor performance.

The work described in this thesis is novel. An extensive literature search revealed no volumetric displays that had been used for real-time presentation of human body motions. Some investigators have made use of the real time capabilities of motion capture systems to provide feedback to the subjects (Hunt et al., 2011; Roosink et al., 2015). Others have used real time visual feedback by displaying live video on a television screen (Malone and Bastian, 2010). Many more motor learning studies use various types of feedback to compare the effectiveness of the different types. For example, McNair et al. compared auditory, instruction, and metaphorical imagery feedback to decrease landing forces (McNair et al., 2000). The display created for this study went a step beyond the feedback of a single variable by showing movement of the human body data volumetrically and simultaneously altering the display color based on the value of the variable being tracked.

6.1 Impact Potential of Display

The volumetric display developed for this thesis has great potential to impact motor learning. The results presented, while collected from only a single test subject, still give insight into the potential for the feedback provided to transform an unwanted movement to the desired one. The expected results previously presented showcase the potential for future motor learning studies to use the applications developed in this thesis.

6.2 Limitations

The display had limitations that should be investigated for future iterations of the display. Finding solutions to these would improve the functionality of the display. The limitations were:

- The data were collected using skin based passive markers that represent the motion of the underlying bones, could be effected by the movement of the soft tissue;
- The real-time capability to import the coordinate data, while marketed as real-time, did take a fraction of a second that caused a slight lag between human motion and display motion;
- The human eye has a refresh rate between 18 and 20 Hz, above this threshold it cannot discern between frames. Ideally, the display would be able to be updated at a rate close to or above the threshold. Saving the intersection data from the real-time trials and playing it back later enabled the display to refresh at ~17 Hz. This provided a smoother motion display compared to the real-time trials. To go above the threshold the coordinate data file, updated at 100 Hz, could be saved and used to update

the image frame by frame. This method would achieve the highest refresh rate while displaying the motion, but it would only be available post trial.

- The array of strings, and the capabilities of the projector limited the distance between the projector and the display. The closer the projector is, the smaller volume that can be displayed in the strings;
- Using a different string layout, potentially determining string locations based on the projector's resolution, could result in a better display with no string dropouts, and a higher density of strings.

6.3 Conclusion and Future Work

This thesis describes the successful creation and interface of a volumetric display with a motion capture system in real time, and showed human movement during three applications for motor learning studies. The test data collected shows how particular variables—moment arm length, trunk lean angle, position error—would change over the course of a trial. This novel volumetric display showed the potential for numerous application in future motor learning studies.

Future work with this project would involve addressing the limitations of the display discussed above. A potential array of strings was created using MATLAB to position strings at increments to not have any bleed over or dropouts (Figure 39). To find the exact layout a display with adjustable strings could be made. The strings could then be positioned based on a projected image of rectangles spaced at intervals that would not

allow bleed over to occur. Since the strings would be adjusted to fit the projected image, there would be no string dropouts either.

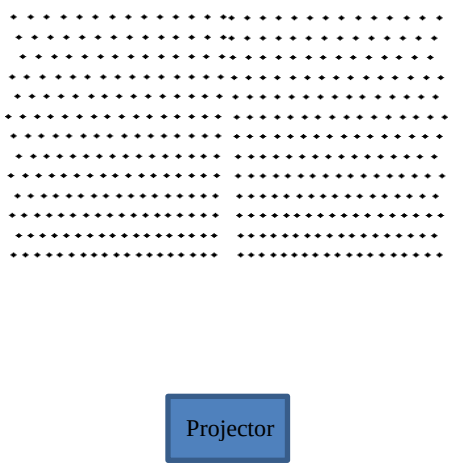

Figure 39: Potential optimal layout made in MATLAB program that positioned each string at an increment of 0.3 radians.

Once these deficiencies have been corrected, the next step would be to conduct a formal motor learning study in which the display is compared with other forms of feedback to determine its comparative effectiveness.

BIBLIOGRAPHY

Aristidou, A., Stavrakis, E., Charalambous, P., Chrysanthou, Y., Himona, S.L., 2015. Folk dance evaluation using Laban Movement Analysis. J. Comput. Cult. Herit. 8, 1–19. doi:10.1145/2755566

Baker, R., 2007. The history of gait analysis before the advent of modern computers. Gait Posture. doi:10.1016/j.gaitpost.2006.10.014

Battini, D., Persona, A., Sgarbossa, F., 2014. Innovative real-time system to integrate ergonomic evaluations into warehouse design and management. Comput. Ind. Eng. 77, 1–10. doi:10.1016/j.cie.2014.08.018

Bordegoni, M., Colombo, G., Formentini, L., 2006. Haptic technologies for the conceptual and validation phases of product design. Comput. Graph. 30, 377–390. doi:10.1016/j.cag.2006.02.012

Brokaw, E.B., Lum, P.S., Cooper, R.A., Brewer, B.R., 2013. Using the kinect to limit abnormal kinematics and compensation strategies during therapy with end effector robots, in: IEEE International Conference on Rehabilitation Robotics. doi:10.1109/ICORR.2013.6650384

Challis, J.H., 1995. A Procedure For Determining Rigid-Body Transformation Parameters. J. Biomech. 28, 733–737.

Dolan, P., Adams, M.A., 1998. Repetitive lifting tasks fatigue the back muscles and increase the bending moment acting on the lumbar spine. J. Biomech. 31, 713–721. doi:10.1016/S0021-9290(98)00086-4

Favalora, G.E., Napoli, J., Hall, D.M., Dorval, R.K., Giovinco, M.G., Richmond, M.J., Chun, W.S., 2002. 100-Million-Voxel Volumetric Display, in: SPIE's 16th Annual International Symposium on Aerospace/Defense Sensing, Simulation, and Controls. doi:10.1117/12.480930

Gray, J.T., Neisser, U., Shapiro, B.A., Kouns, S., 2002. Observational Learning of Ballet Sequences: The Role of Kinematic Information. Ecol. Psychol. 1–15.

Guglielmelli, E., Micera, S., Migliavacca, F., Pedotti, A., 2015. Moving Along. IEEE Pulse 12, 49–57.

Horn, R.R., Williams, A.M., Scott, M. a, Hodges, N.J., 2005. Visual search and coordination changes in response to video and point-light demonstrations without KR. J. Mot. Behav. 37, 265–274.

Hunt, M. a., Simic, M., Hinman, R.S., Bennell, K.L., Wrigley, T. V., 2011. Feasibility of a gait retraining strategy for reducing knee joint loading: Increased trunk lean guided by real-time biofeedback. J. Biomech. 44, 943–947. doi:10.1016/j.jbiomech.2010.11.027

Hunt, M.A., 2013. Movement retraining using real-time feedback of performance. J. Vis. Exp. e50182. doi:10.3791/50182

Jing, C.L., Feng, Q. Bin, Zhang, Y.S., Yang, G.L., Song, Z.G., Pei, Z.Q., Lv, G.Q., 2014. LED-Based 3-DMD Volumetric 3D Display. Appl. Mech. Mater. 596, 442–445. doi:10.4028/www.scientific.net/AMM.596.442

Kernodle, M.W., Carlton, L.G., 1992. Information feedback and the learning multiple-degree-of-freedom activities. J Mot Behav 24, 187–196. doi:10.1080/00222895.1992.9941614

Kernozek, T., Iwasaki, M., Fater, D., Durall, C., 2006. Movement-basedfeedbackmayreduce spinalmomentsinmaleworkersduring liftandloweringtasks. Physiother. Res. Int.Ltd Physiother. Physiother. Res. Int. Physiother. Res. Int 1111. doi:10.1002/pri

Kilteni, K., Normand, J.M., Sanchez-Vives, M. V., Slater, M., 2012. Extending body space in immersive virtual reality: A very long arm illusion. PLoS One 7. doi:10.1371/journal.pone.0040867

Kim, J., Gravunder, A., Park, H.-S., 2015. Commercial Motion Sensor Based Low-Cost and Convenient Interactive Treadmill. Sensors (Basel). 15, 23667–83. doi:10.3390/s150923667

Krishnan, C., Washabaugh, E.P., Seetharaman, Y., 2015. A low cost real-time motion tracking approach using webcam technology. J. Biomech. 48, 544–548. doi:10.1016/j.jbiomech.2014.11.048

Kurillo, G., Han, J.J., Abresch, R.T., Nicorici, A., Yan, P., Bajcsy, R., 2012. Development and Application of Stereo Camera-Based Upper Extremity Workspace Evaluation in Patients with Neuromuscular Diseases. PLoS One 7. doi:10.1371/journal.pone.0045341

Lajoie, Y., 2004. Effect of computerized feedback postural training on posture and attentional demands in older adults. Aging Clin. Exp. Res. 16, 363–368. doi:http://www.ncbi.nlm.nih.gov/entrez/query.fcgi?cmd=Retrieve&db=PubMed&dopt=Citation&list_uids=15636461

Langhans, K., Guill, C., 2003. SOLID FELIX: A static volume 3D-laser display. Electron. … 5006, 161–174. doi:10.1117/12.474155

Lavender, S.A., Lorenz, E., Andersson, G.B.J., 2002. Training in Lifting. Prof. Saf. 30–35.

Lee, S., Park, S., Chung, K., Cho, C., 2015. Kinematic skeleton based control of a virtual simulator for military training. Symmetry (Basel). 7, 1043–1060. doi:10.3390/sym7021043

Mäkinen, T.M., Rintamäki, H., Korpelainen, J.T., Kampman, V., Pääkkönen, T., Oksa, J., Palinkas, L.A., Leppäluoto, J., Hassi, J., 2005. Postural sway during single and repeated cold exposures. Aviat. Sp. Environ. Med. 76, 947–953.

Malone, L.A., Bastian, A.J., 2010. Thinking about walking: effects of conscious correction versus distraction on locomotor adaptation. J. Neurophysiol. 103, 1954–62. doi:10.1152/jn.00832.2009

Manchikanti, L., Singh, V., Falco, F.J.E., Benyamin, R.M., Hirsch, J.A., 2014. Epidemiology of Low Back Pain in Adults. Neuromodulation Technol. Neural Interface 17, 3–10. doi:10.1111/ner.12018

McNair, P.J., Prapavessis, H., Callender, K., 2000. Decreasing landing forces: effect of instruction., British journal of sports medicine. doi:10.1136/bjsm.34.4.293

Muybridge, E., 1907. The Human Figure in Motion - An Electro Phothographic Investigation of Consecutive Phases of Muscular Actions.

Normand, J.M., Giannopoulos, E., Spanlang, B., Slater, M., 2011. Multisensory stimulation can induce an illusion of larger belly size in immersive virtual reality. PLoS One 6. doi:10.1371/journal.pone.0016128

O'Malley, M.K., Gupta, A., 2008. Haptic Interfaces, HCI Beyond the GUI. doi:10.1016/B978-0-12-374017-5.00002-X

Patel, K., Bailenson, J.N., Jung, S.-H., Diankov, R., Bajcsy, R., 2006. PRESENCE 2006 The Effects of Fully Immersive Virtual Reality on the Learning of Physical Tasks Kayur Patel University of Washington University of California at Berkeley. Proc. 9th Annu. Int. Work. Presence 129–138.

Portnoy, S., Halaby, O., Dekel-Chen, D., Dierick, F., 2015. Effect of an auditory feedback substitution, tactilo-kinesthetic, or visual feedback on kinematics of pouring water from kettle into cup. Appl. Ergon. 51, 44–49. doi:10.1016/j.apergo.2015.04.008

Roosink, M., Robitaille, N., McFadyen, B.J., Hébert, L.J., Jackson, P.L., Bouyer, L.J., Mercier, C., 2015. Real-time modulation of visual feedback on human full-body movements in a virtual mirror : development and proof-of-concept. J. Neuroeng. Rehabil. 12, 1–10. doi:10.1186/1743-0003-12-2

Sadowski, J., Mastalerz, A., Niźnikowski, T., Wiśniowski, W., Biegajło, M., Kulik, M., 2011. The Effects of Differnt Types of Verbal Feedback on Learning a Complex Movement Task. J. Sport Tour. 18, 300–307. doi:10.2478/v10197-011-0026-2

Schubiger-Banz, S., Eberle, M., 2008. The NOVA Display System 7, 476–487.

Shumway-Cook, A., Anson, D., Haller, S., 1988. Postural sway biofeedback: its effect on

reestablishing stance stability in hemiplegic patients. Arch. Phys. Med. Rehabil. 69, 395–400.

Sigrist, R., Rauter, G., Riener, R., Wolf, P., 2013. Augmented visual, auditory, haptic, and multimodal feedback in motor learning: A review. Psychon. Bull. Rev. 20, 21–53. doi:10.3758/s13423-012-0333-8

Sigrist, R., Schellenberg, J., Rauter, G., Broggi, S., Riener, R., Wolf, P., 2011. Visual and Auditory Augmented Concurrent Feedback in a Complex Motor Task. Presence Teleoperators Virtual Environ. 20, 15–32. doi:10.1162/pres_a_00032

Swan, L., Otani, H., Loubert, P. V., 2007. Reducing postural sway by manipulating the difficulty levels of a cognitive task and a balance task. Gait Posture 26, 470–474. doi:10.1016/j.gaitpost.2006.11.201

Willy, R.W., Davis, I.S., 2013. Varied response to mirror gait retraining of gluteus medius control, hip kinematics, pain, and function in 2 female runners with patellofemoral pain. J Ortho Sport. Phys Ther 43, 864–74. doi:10.2519/jospt.2013.4516

Zhang, Z., 2012. Microsoft kinect sensor and its effect. IEEE Multimed. 19, 4–10. doi:10.1109/MMUL.2012.24